Received: 4 October 2021 | Revised: 2 November 2021 | Accepted: 2 November 2021

DOI: 10.1111/gcb.16023

Global Change Biology WILEY

PRIMARY RESEARCH ARTICLE

Beyond bulk: Density fractions explain heterogeneity in global soil carbon abundance and persistence

Katherine Heckman[1] | Caitlin E. Hicks Pries[2] | Corey R. Lawrence[3] | Craig Rasmussen[4] | Susan E. Crow[5] | Alison M. Hoyt[6,7] | Sophie F. von Fromm[6,8] | Zheng Shi[9] | Shane Stoner[6,8] | Casey McGrath[5] | Jeffrey Beem-Miller[6] | Asmeret Asefaw Berhe[10] | Joseph C. Blankinship[4] | Marco Keiluweit[11] | Erika Marín-Spiotta[12] | J. Grey Monroe[13] | Alain F. Plante[14] | Joshua Schimel[15] | Carlos A. Sierra[6,16] | Aaron Thompson[17] | Rota Wagai[18]

[1]USDA Forest Service, Northern Research Station, Houghton, Michigan, USA

[2]Department of Biological Sciences, Dartmouth College, Hanover, New Hampshire, USA

[3]U.S. Geological Survey, Geosciences and Environmental Change Science Center, Denver, Colorado, USA

[4]Department of Environmental Science, University of Arizona, Tucson, Arizona, USA

[5]Natural Resources and Environmental Management Department, University of Hawaii Manoa, Honolulu, Hawaii, USA

[6]Department of Biogeochemical Processes, Max-Planck-Institute for Biogeochemistry, Jena, Germany

[7]Climate and Ecosystem Sciences Division, Lawrence Berkeley National Laboratory, Berkeley, California, USA

[8]Department of Environmental Systems Science, ETH Zurich, Zurich, Switzerland

[9]Computational Sciences & Engineering Division and Climate Change Science Institute, Oak Ridge National Laboratory, Oak Ridge, Tennessee, USA

[10]Department of Life and Environmental Sciences, University of California, Merced, California, USA

[11]School of Earth & Sustainability and Stockbridge School of Agriculture, University of Massachusetts, Amherst, Massachusetts, USA

[12]Department of Geography, University of Wisconsin-Madison, Madison, Wisconsin, USA

[13]Department of Plant Sciences, University of California, Davis, Davis, California, USA

[14]Department of Earth & Environmental Science, University of Pennsylvania, Philadelphia, PA, USA

[15]Department of Ecology Evolution and Marine Biology, University of California Santa Barbara, Santa Barbara, California, USA

[16]Department of Ecology, Swedish University of Agricultural Sciences, Uppsala, Sweden

[17]Department of Crop and Soil Sciences and the Odum School of Ecology, University of Georgia, Athens, Georgia, USA

[18]Institute for Agro-Environmental Sciences, National Agriculture and Food Research Organization, Tsukuba, Ibaraki, Japan

Correspondence
Katherine Heckman, 410 MacInnes Drive, Houghton, MI 49931, USA.
Email: katherine.a.heckman@usda.gov

Caitlin Hicks Pries, 78 College Street, Hanover, NH 03755, USA.
Email: Caitlin.Hicks.Pries@dartmouth.edu

Funding information
U.S. Geological Survey John Wesley Powell Center; Max Planck Institute for Biogeochemistry, Grant/Award Number: 695101; U.S. Department of Agriculture, Grant/Award Number: 2018-67003-27935; U.S. Geological Survey

Abstract

Understanding the controls on the amount and persistence of soil organic carbon (C) is essential for predicting its sensitivity to global change. The response may depend on whether C is unprotected, isolated within aggregates, or protected from decomposition by mineral associations. Here, we present a global synthesis of the relative influence of environmental factors on soil organic C partitioning among pools, abundance in each pool (mg C g^{-1} soil), and persistence (as approximated by radiocarbon abundance) in relatively unprotected particulate and protected mineral-bound pools. We show that C within particulate and mineral-associated pools consistently

Katherine Heckman and Caitlin E. Hicks Pries share first author status.

differed from one another in degree of persistence and relationship to environmental factors. Soil depth was the best predictor of C abundance and persistence, though it accounted for more variance in persistence. Persistence of all C pools decreased with increasing mean annual temperature (MAT) throughout the soil profile, whereas persistence increased with increasing wetness index (MAP/PET) in subsurface soils (30–176 cm). The relationship of C abundance (mg C g^{-1} soil) to climate varied among pools and with depth. Mineral-associated C in surface soils (<30 cm) increased more strongly with increasing wetness index than the free particulate C, but both pools showed attenuated responses to the wetness index at depth. Overall, these relationships suggest a strong influence of climate on soil C properties, and a potential loss of soil C from protected pools in areas with decreasing wetness. Relative persistence and abundance of C pools varied significantly among land cover types and soil parent material lithologies. This variability in each pool's relationship to environmental factors suggests that not all soil organic C is equally vulnerable to global change. Therefore, projections of future soil organic C based on patterns and responses of bulk soil organic C may be misleading.

KEYWORDS
climate change, persistence, radiocarbon, soil carbon, soil fractions, soil organic matter, terrestrial carbon cycle

1 | INTRODUCTION

Investigations into the controls on soil organic carbon (C) have often treated it as a single homogeneous pool (e.g., Rasmussen et al., 2018; Shi et al., 2020). However, decades of research have emphasized the heterogeneity of soil organic C (Ågren & Bosatta, 1996; Hénin & Dupuis, 1945; Swift et al., 1979; Trumbore, 2009). Soils have a range of C pools cycling at different timescales, making estimates of soil organic C persistence based on bulk $\Delta^{14}C$ values misleading (Gaudinski et al., 2000; Trumbore & Zheng, 1996). Improving how we parameterize terrestrial C models to better predict global C dynamics requires building a better understanding of the environmental factors that control the size and distribution of these active and passive C pools (Blankinship et al., 2018; Davidson & Janssens, 2006). Understanding the relationship between the physical environment and the partitioning of C among these pools will also be important if we are to develop strategies to improve soil health and estimate the potential for C sequestration to mitigate climate change (Bongiorno et al., 2019).

Therefore, to better understand the response of soil organic C to global change, it is important to go "beyond bulk C" and consider whether distinct functional C pools are regulated by the same, similar, or unique soil forming factors on a global scale. At the broadest conceptual scale, the critical "soil forming factors" that regulate soil organic C stabilization include climate (*cl*), organisms (*o*), and relief (*r*) modifying soil parent material (*p*) through inputs and weathering reactions over time (*t*; referred to as the "*cl*,*o*,*r*,*p*,*t*" soil forming factors; Dokuchaev, 1883; Jenny, 1941). However, assigning quantitative measures of the influence of these soil forming factors on soil organic C abundance and persistence (Sierra et al., 2018) has been hampered by the heterogeneous nature of soil organic C and the complexity of the interactions among soil forming factors.

Soil organic C decomposition rates comprise a spectrum ranging from hours to millennia. Likewise, the molecular composition of soil organic C varies widely based on source, degree of decomposition, and association with soil minerals and within soil aggregates. Although there are approaches to model the continuum of decomposition rates of soil organic C (Ågren & Bosatta, 1996; Carpenter, 1981), models often partition this continuum of rates into a few discrete categories or pools (Elliott et al., 1996; Sierra et al., 2012). Pools that exhibit true mechanistic differences may not be physically measurable. However, the wide variation in the criteria used to evaluate these pools (e.g., radiocarbon, incubation, fractionation) is often used as evidence that bulk soil contains multiple pools that exhibit distinct dynamics (Baisden & Canessa, 2013; Buchkowski et al., 2019; Cotrufo et al., 2013). As there is increasing evidence that radiocarbon data can be used to constrain global soil C models (e.g., He et al., 2016a), it is essential that we test whether our measurements of these pools align with their conceptual representation in our models (Blankinship et al., 2018).

Our current conceptual understanding of soil organic C cycling divides bulk organic C into pools directly associated with specific mechanisms and processes that affect its decomposition rate, including mineral sorption, aggregation, and microbial accessibility. In practice, laboratory studies separate bulk soil organic C into operationally defined fractions that differ based on physical, biological, or

chemical properties and are associated with specific mechanisms of stabilization (Baisden et al., 2002; Golchin et al., 1994; Jastrow et al., 1996; Six et al., 2000; Swanston et al., 2005; Trumbore & Zheng, 1996). For example, density fractionation isolates soil organic C into free particulate, occluded particulate, and mineral-associated fractions (Figure S1; Greenland, 1964; Heckman et al., 2014; Lavallee et al., 2020; Sollins et al., 1999; Spycher et al., 1983) that are hypothesized to align with current conceptual pools associated with different stabilization mechanisms (Cotrufo et al., 2019).

In this study, we use a global synthesis of soil radiocarbon data (Beem-Miller et al., 2021; Lawrence et al., 2020) to evaluate whether the three common fractions isolated through density fractionation methods (Figure S1; Golchin et al., 1994) exhibit distinct relationships with soil forming factors at the global scale. The free particulate fraction (also known as the free light fraction) includes particulate organics and any material not bound to minerals or occluded in aggregates; this fraction floats in a dense liquid (most commonly sodium polytungstate). Conceptually, this fraction is the most microbially available and the least persistent of the fractions (excepting dissolved C, which is not captured in traditional density fractionation methods), corresponding to an actively metabolized or fast-cycling pool in models. The particulate occluded fraction (also known as the occluded light fraction)—composed of particulate organic matter released after vigorous mixing and ultrasonic disruption of soil aggregates—is assumed to be physically protected from microbial access through occlusion in aggregates. However, the makeup of these aggregates is often heterogeneous (Marín-Spiotta et al., 2008) and may include organic C with high molecular stability such as pyrogenic C, phytoliths, and fungal spores (Wagai et al., 2009). Conceptually, the particulate occluded fraction may be protected by physical isolation or molecular recalcitrance (as defined by structural resistance to enzymatic attack or poor microbial substrate quality) and is commonly thought to cycle at intermediate rates (Golchin et al., 1994; Wagai et al., 2009). After isolation of these two particulate fractions, organic matter remaining is associated with the mineral fraction (sometimes referred to as the dense or heavy fraction) and is assumed to be adsorbed to, co-precipitated with, or reside in microaggregate structures with minerals (Wagai et al., 2020). We refer to this fraction as mineral-associated C. Conceptually, mineral-associated C is the pool most protected from microbial decomposition, corresponding to a more slowly cycling C pool. In certain soils and ecosystems, the characteristics of these fractions have been successfully linked to specific stabilization mechanisms (von Lützow et al., 2007). However, the global applicability of these fractions to conceptual C pools and the influence of environmental factors on these soil organic C fractions are poorly resolved.

The response of soil organic C to our changing climate is uncertain in Earth system models (Shi et al., 2018; Todd-Brown et al., 2018); as a result, modelers place low confidence on soil organic C response projections (Bradford et al., 2016; Davidson & Janssens, 2006; Friedlingstein et al., 2014). One source of uncertainty in modeling soil organic C dynamics is the complete lack of—or otherwise inconsistent treatment of—within-soil variance in decomposition rate. Though many models are structured with multiple soil organic C pools, global-scale models are often validated with bulk soil C data (e.g., from the Harmonized World Soils Database). Research has concluded that the mean age of bulk soil C is hundreds to thousands of years (He et al., 2016b; Shi et al., 2020; Sierra et al., 2018). From a climate change perspective, the potential of soils to sequester CO_2 may therefore be limited by the slow assimilation rates of new inputs or the development of new reactive secondary mineral phases (Schlesinger, 1990). To determine soil C dynamics on the timescale of anthropogenic climate change, information about the full spectrum of soil C pools and their associated decomposition rates would be beneficial. In particular, soil organic C dynamics under climate change are likely determined by the active and intermediate (e.g., particulate) pools which may be more responsive to changes in inputs (Crow & Sierra, 2018; Knorr et al., 2005; Shi et al., 2020; Soong et al., 2021). Better understanding of these intermediate pools could improve our ability to manage both C inputs and C persistence to maximize the climate benefit of C sequestration (Crow & Sierra, 2018; Sanderman et al., 2017; Sierra et al., 2021; Van Gestel et al., 2018). Furthermore, we could develop more effective pathways to sequester C by identifying management practices that encourage greater C stabilization and slower rates of soil organic mineralization. However, prior to identifying these management techniques, it is essential to establish a firm understanding of what controls the partitioning of soil organic C into pools and governs C persistence within those pools.

Here, we assess the relationship of soil forming factors to the partitioning and persistence of soil organic C fractions in free particulate, occluded particulate, and mineral-associated fractions. We hypothesize that fractions respond differently to climate, vegetation, and physicochemical parameters due to differences in how they are formed and protected from soil microbes. For example, we hypothesize that the unprotected free particulate fraction should decrease in response to increasing mean annual temperature and the associated increase in microbial activity; in contrast, we hypothesize that the more protected occluded and mineral-associated fractions should have no relationship to temperature because microbial access, not activity, limits their decomposition. The relationships of the fractions with soil forming factors can offer insights into the sensitivity of soil C to global changes.

2 | METHODS

We used soil density fraction data from The International Soil Radiocarbon Database (ISRaD v. 1.1.2 Lawrence et al., 2020; www.soilradiocarbon.org). ISRaD is an online repository for environmental radiocarbon data with a specific emphasis on soils and soil fractions. We utilized a subset of ISRaD data comprising measurements of radiocarbon (persistence), organic C concentration (abundance), or the proportion of organic C in the mineral-associated fraction (distribution) made on soil density fractions for the current analysis. Radiocarbon data are reported in units of $\Delta^{14}C$ (‰) normalized to

account for the year of sampling (Shi et al., 2020; see below). In studies that employed sequential density separation (isolation of multiple free light, occluded light, and heavy fractions for the same sample), the multiple fractions were combined by taking a mass-weighted average for C abundance and C-weighted average for $\Delta^{14}C$ values. C distribution among density fractions was normalized to sum to 100%. Overall, our meta-analysis included data from 52 studies. In addition to C measurements, ISRaD compiles ancillary data regarding site and sample characteristics that were either provided directly in the associated published works or provided as supplementary information from manuscript authors.

First, we compared the general characteristics of the three density fractions using a linear mixed model (LMM) with fraction as a fixed effect and the sampled layer nested in the study as a random effect because fractions measured within a soil sample are not independent nor are samples measured within the same study. We then used the emmeans (Lenth, 2019) package to perform post hoc pairwise Tukey tests of differences between the fractions. Second, we used LMMs to explore how soil fractions interact with environmental predictors related to soil forming factors to affect C abundance, persistence, and distribution at a global scale (Figure S2). We chose the LMM approach so that we could explicitly include interactions among the soil fractions and environmental predictors.

For the radiocarbon data from the ISRaD, each $\Delta^{14}C$ measurement was normalized to the year 2000 using a steady state one-pool model and the observed time series of atmospheric $\Delta^{14}C$ according to Shi et al. (2020). Steady state conditions assume constant inputs through time; therefore, input does not affect the result of normalization. Past atmospheric $\Delta^{14}C$ records were obtained from the Intcal13 calibration curve (50 kyr – 0 BP; Reimer et al., 2013). Modern data from 1950 were obtained from Vermunt and Schauinsland stations (Levin & Kromer, 1997) extended through 2012 (Hua et al., 2013; Levin et al., 2013). To normalize $\Delta^{14}C$ from the year of sampling to year 2000, we first constructed the relationship between turnover time and $\Delta^{14}C$ to derive a turnover time for each $\Delta^{14}C$ value. Then we adjusted the original $\Delta^{14}C$ value by running the one-pool model with the respective turnover time to year 2000. When $\Delta^{14}C$ is greater than about 85‰, the calculation generates two mean turnover times; the longer turnover times were used.

2.1 | Explanatory variables

The explanatory environmental variables used in the meta-analysis were grouped according to the soil forming factors (Jenny, 1941): climate, organisms, relief, and parent material. The specific variables included mean annual temperature (MAT), wetness index (MAP/PET), net primary productivity (NPP), land cover type, elevation, slope, northness, and parent material (Table 1). The influence of time on the degree of soil morphological development was not explicitly included in this analysis due to the difficulty of determining

TABLE 1 The source of the environmental predictors representing CLORPT soil forming factors used in our analyses

CLORPT factor	Model predictor	Unit	Calculation	Source	Resolution
Climate	Mean annual temperature (MAT)	°C		WorldClim 2.1	1 km
	Wetness index	Ratio, mm mm^{-1}	Mean annual precipitation (MAP)/Potential evapotranspiration (PET)	WorldClim 2.1 (MAP), Global Aridity Index and Potential Evapotranspiration Climate Database v2 (PET)	1 km (MAP), 30 arc-seconds (PET)
Organisms	Net primary productivity	kg C m^{-2}	Mean of values from 2001–2016	MODIS/Terra	500 m
	Land cover	Factor		Reported in study, gap-filled with MODIS/Terra + Aqua	500 m
Relief	Elevation	m		DEM (World Elevation Terrain): Esri Living Atlas	30 m
	Slope	%		DEM (World Elevation Terrain): Esri Living Atlas	30 m
	Northness	−1 (equator-facing) to 1 (pole-facing)	cos(aspect)*sin(slope), adjusted so −1 is equator facing	DEM (World Elevation Terrain): Esri Living Atlas	30 m
Parent Material	Parent material	Factor		Reported in study, expert opinion	
Time	NA				

approximate soil ages. Along with the soil forming factors described above, we included fraction (for $\Delta^{14}C$ and C abundance models only) and depth as predictors. Depth referred to the middle of each increment sampled to integrate across the various sampling approaches used. The top of the mineral soil was set to 0 cm following soil science convention. When directly reported information on these variables was available in ISRaD, it was used. When variables of interest were not available directly through ISRaD, these variables were populated through utilization of geolocated databases (Table 1; Supporting Information).

As is the nature of meta-analyses, our dataset is limited by the availability of soil fraction data that include radiocarbon values (Figures S2). We evaluated the distribution of MAT, wetness index, NPP, slope, and elevation in our dataset against their respective global distributions (Figure S3). The dataset represents the global distribution of these variables well except for flat regions (note that very cold regions are mostly from Antarctica and circumpolar regions which likely do not have soil, Figure S3g). However, the dataset is skewed toward the northern hemisphere and temperate forests, where the majority of soil density fractionation studies have been carried out (Figures S2–S4). The full compiled dataset used in the current analysis is available in the supplementary materials. For a detailed description of explanatory variable extraction/origin, please see supplementary materials.

2.2 | Linear mixed-effects models

We ran mixed model multiple regressions using the lmer command from lme4 (Bates et al., 2014) in R v. 3.5.3 3 (R Core Team, 2020) to determine the relationships between soil forming factors, depth, and soil fraction, and the three response variables: normalized $\Delta^{14}C$ values (‰), the abundance of organic C in each fraction (in mg C per g soil), and the proportion of organic C stored in the heavy fraction. We report the results of the final models with *p*-values calculated using the lmerTest package (Kuznetsova et al., 2016) and the marginal and conditional R^2 values computed using the "r.squaredGLMM" function from the MuMIN package (Bartoń, 2019). We report *F*-test statistics as a relative measure of the amount of variance explained by each fixed effect while taking into account the degrees of freedom. Where possible (e.g., where interactions were not missing certain combinations), we further explored statistically significant interactions using post hoc tests of the estimated marginal means using the emmeans package (Lenth, 2019). We present the results from models for which we optimized the random effects structure using Akaike's information criterion (AIC) and tested for violations of homogeneity of variance and linearity assumptions. We limited our analyses to data from soil depths <300 cm because below that depth the relationships between our response variables and depth became nonlinear. We checked for multicollinearity among our continuous predictors and did not include any pairs of predictors that had a correlation value (r) > 0.6 (Dormann et al., 2013; Figure S5). We used centered and scaled continuous variables in the model to reduce the multicollinearity that can occur with interaction terms. However, we graphically present the predicted relationships between our response variables and soil forming factors using unscaled and uncentred explanatory variables and untransformed response variables to better illustrate their actual effects. The predicted lines were calculated based on the LMM using the "ggpredict" function from the ggeffects package (Lüdecke, 2018) and represent the relationship between the response variable and a continuous predictor of interest with other continuous predictors set to their means and the land cover and parent material factors set to temperate forest and igneous intrusive, respectively.

We chose which interactions to include in our model based on a priori hypotheses and graphical exploration. Based on a priori hypotheses, we included two-way interactions between wetness index × slope (due to the dependence of infiltration and erosion on slope), wetness index × parent material (due to the differential weathering rates of different lithologies), fraction × parent material (because we expect lithology to have a stronger effect on the mineral-associated fraction), and two- and three-way interactions among MAT × fraction × depth (because we expect temperature sensitivity may differ among soil fractions and depths) and wetness index × fraction × depth (moisture influences transport of organics and mineral phases with depth in the profile). Based on graphical exploration of the relationships of response variables to soil forming predictors by fraction (e.g., Figures S8 and S12), we also included the two-way interactions of fraction × land cover and fraction × slope.

To optimize the random effect structure, we ran our full model (all predictors and the interactions described above) for $\Delta^{14}C$, the response variable for which we had the most data ($n = 1323$) using the lmer command (lme4 package) in R (R Core Team, 2020). The random effects tested included a random slope of the depth effect based on the soil pedon, random intercepts based on the study (entry_name in ISRaD), the soil pedon nested within study, the soil layer nested within study, and the soil layer nested within the soil pedon. Combinations of these random effects were compared using AIC and the model with the lowest AIC was chosen. The best-fit model had a random slope of the depth effect based on the soil pedon and random intercepts of the soil layer nested within the study. Thus, the model accounted for the relationship between $\Delta^{14}C$ and depth varying by the soil core or pit, the fact that the fractions sampled were not independent (they were derived from the same soil layer), and the lack of independence among soil layers from the same study.

Next, we ran the full model with the optimum random effects and graphed residuals versus all the predictors to test whether the assumption of variance homogeneity was violated, which it was because variance increased with soil depth. The lmer function does not have an argument to handle variance heterogeneity. Thus, in consultation with a developer of lme4 (Dr. Benjamin Bolker, McMaster University, written communication, March 3, 2020), we chose to account for variance homogeneity by creating an observation level random effect that interacts with a dummy value for quantiles of depth (2.5–5.5 cm, 5.5–10 cm, 10–19 cm, 19–37.5 cm, 37.5–67.5 cm, and 67.5–176 cm) excluding the shallowest

depth quantile, which had the lowest variance. Graphing residuals demonstrated that this approach reduced variance heterogeneity. Lastly, we graphed partial residuals to ensure that the relationships between our response variables and continuous predictors were linear. Satisfied that the assumptions of linear models were met, we proceeded to the final full model, which included all explanatory variables, the chosen interaction terms, the random effect structure with the smallest AIC, and the dummy values to account for depth heterogeneity.

We followed the same procedure for the C abundance in the various fractions ($n = 981$) and used the same random effects structure as the $\Delta^{14}C$ model. The C abundance model did not need a variance structure, but the responses were log transformed to meet the assumption of linearity. The proportion of C in the heavy fraction model ($n = 457$) also did not need a variance structure, but the responses were logit transformed and the depth predictor was log transformed to meet assumptions of linearity.

3 | RESULTS

We found consistent and significant differences in density fraction characteristics at the global scale (Table 2; Figure 1). On average, mineral-associated fractions had the lowest C concentrations (2.3 ± 0.2%) but had the greatest C abundance (17.4 ± 1.2 mg g^{-1} soil) due to their high mass compared to free and occluded particulate fractions ($p < .0001$). Soils stored almost 60% of their organic C in mineral fractions, whereas only 14% was stored in occluded fractions ($p < .0001$). Occluded particulate fractions had the highest C:N (32 ± 0.2) while mineral-associated fractions had the lowest C:N (13 ± 1; $p < .0001$). The free particulate fraction was similar to occluded fraction in $\delta^{13}C$ (−25.2 ± 0.2‰ vs. −25.5 ± 0.2‰) but was the most depleted (smaller values) in $\delta^{15}N$ (1.2 ± 0.2‰), while the mineral-associated fraction was the most enriched (−23.8 ± 0.2‰ and 4.4 ± 0.2‰; $p < .0001$ for both). Lastly, the free particulate fraction had significantly younger $\Delta^{14}C$ values (6.2 ± 7.5) than the occluded particulate or mineral-associated fractions ($p < .0001$), whose $\Delta^{14}C$ (‰) did not differ significantly from one another (−50.9 ± 12.6 and −79.4 ± 8.0, respectively; $p = .58$).

TABLE 2 General characteristics of density fractions. Values are means with parenthetical standard errors. Letters indicate statistically significant differences ($p < .05$) among fractions which were determined by running a linear mixed model including random effects followed by type III effects tests ($\alpha = 0.05$). All fractions were significantly different from one another, except for $\Delta^{14}C$ where occluded particulate and mineral-associated fractions did not differ ($p = .58$)

	Free particulate	Occluded particulate	Mineral-associated
%C ($n = 1528$)	24.5 (0.5)^{b}	34.4 (0.4)^{a}	2.3 (0.2)^{c}
mg C g^{-1} soil ($n = 981$)	9.9 (0.8)^{b}	6.1 (0.8)^{c}	17.4 (1.2)^{a}
C/N ($n = 932$)	29 (1)^{b}	32 (0.2)^{a}	13 (<1)^{c}
Proportion of total C (%) ($n = 1222$)	33 (1)^{b}	14 (1)^{c}	59 (1)^{a}
$\delta^{15}N$ (‰) ($n = 672$)	1.2 (0.2)^{c}	3.2 (0.2)^{b}	4.4 (0.2)^{a}
$\delta^{13}C$ (‰) ($n = 1291$)	−25.2 (0.2)^{b}	−25.5 (0.2)^{c}	−23.8 (0.2)^{a}
$\Delta^{14}C$ (‰) ($n = 1399$)	6.2 (7.5)^{a}	−50.9 (12.6)^{b}	−79.4 (8.0)^{b}

Overall, our LMMs using soil forming factors, depth, and fraction as predictors explained over half the variation in $\Delta^{14}C$ (‰) and C abundance (mg C g^{-1} soil; marginal $R^2 = 0.60$ and 0.59, respectively; Figures 2 and 3). Depth and fraction type explained the largest amount of variation in both models according to their F values, though depth had a much higher explanatory power for $\Delta^{14}C$. However, our LMM using soil forming factors and depth as predictors explained less than half the variation in the proportion of C associated with the heavy fraction (marginal $R^2 = 0.40$; Figure S6). The relative significance of soil forming factors varied slightly among models depending on the response variable. Detailed results for each model are given below.

3.1 | C persistence (normalized $\Delta^{14}C$)

Depth explained the largest amount of variation in our $\Delta^{14}C$ model ($F = 368$; $p < .001$). As expected, soil fraction was a significant predictor in our $\Delta^{14}C$ model ($F = 25$, $p < .001$) and significantly interacted with depth (fraction × depth, $F = 8$, $p = .0004$, Figure 4). Carbon persistence increased with depth as $\Delta^{14}C$ became more depleted, and this effect of depth was stronger in the occluded particulate and mineral-associated fractions than in the free particulate fraction (Figure 4). Though soil forming factors explained smaller portions of variance, several significant relationships with climate variables were noted. Contrary to our hypothesis, C persistence decreased ($\Delta^{14}C$ became more enriched) as MAT increased in all fractions (MAT, $F = 5$, $p = .035$; Figure S7). In general, soil $\Delta^{14}C$ was more depleted in humid ecosystems than in dry ecosystems. The influence of wetness index on $\Delta^{14}C$ increased with increasing depth (depth × wetness index, $F = 9$, $p = .003$), indicating a stronger response to moisture in the subsurface (Figure 5).

Carbon persistence generally varied among fractions within a land cover type (fraction × land cover, $F = 8$, $p < .001$; Figure S8). The mineral-associated and the occluded fractions had higher C persistence than the free particulate fraction in most land covers. The only exceptions were tropical forests and tundra ($p > .23$), which showed a similar C persistence between the mineral-associated and the free particulate fractions, and shrublands and tropical forests, which showed no differences between the occluded and the free light fractions ($p > .81$). Carbon persistence differed between mineral-associated and occluded particulate fractions only in boreal forests, shrublands, and croplands ($p < .025$). Croplands had the least persistent occluded particulate fraction; significantly younger than the occluded fraction in grasslands, shrublands, and temperate and tropical forests ($p < .055$).

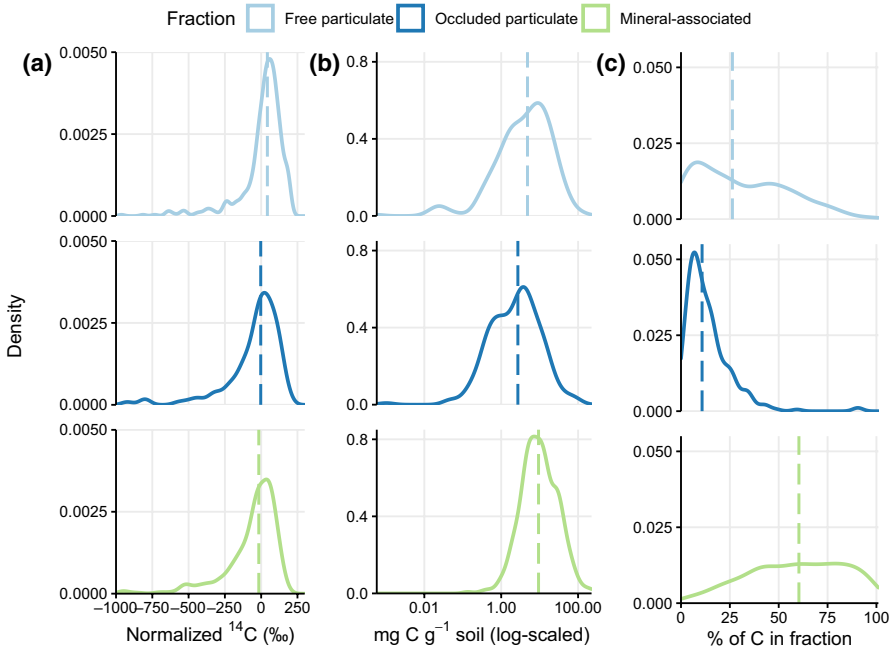

FIGURE 1 Density distribution of (a) normalized $\Delta^{14}C$, (b) C abundance, and (c) percent (%) distribution of C among fractions. Dashed vertical lines correspond to the median value for each group, respectively [Colour figure can be viewed at wileyonlinelibrary.com]

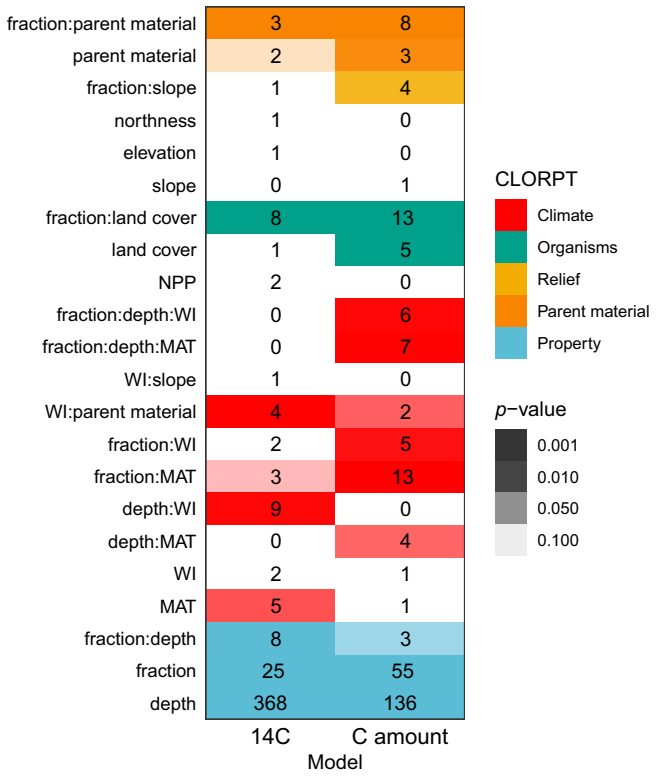

FIGURE 2 Summary statistics for two mixed models assessing the influence of soil forming factors on $\Delta^{14}C$ and C (mg g^{-1}) of soil organic matter fractions colored by soil forming factor, where "Property" refers to soil fraction and depth, with color shade scaled by *p*-value and labeled with *F*-values. For $\Delta^{14}C$ model, $n = 1323$, marginal $R^2 = 0.60$, conditional $R^2 = 0.98$. For C amount model, $n = 981$, marginal $R^2 = 0.59$, conditional $R^2 = 0.79$ [Colour figure can be viewed at wileyonlinelibrary.com]

There were several significant differences in the relationships of the fractions to one another within parent material classes (fraction × parent material, $F = 3$, $p < .001$; Figure S9), and the influence of parent material on C persistence varied with wetness index (parent material × wetness index, $F = 4$, $p < .001$; Figure S10). Soils developed from igneous extrusive, igneous pyroclastic, and sedimentary-clastic parent materials increased in C persistence with increasing moisture across the sampled range of wetness index values, while other parent materials did not (0.25–1.75).

3.2 | C abundance (mg C g^{-1} soil)

As with C persistence, depth explained the most variation in C abundance ($F = 136$, $p < .001$), followed by fraction type ($F = 55$, $p < .001$); again, there was a significant fraction by depth interaction (fraction × depth, $F = 3.1$, $p = .04$). While soil forming factors explained lesser portions of variance, the climate variables, MAT, and wetness index, as well as land cover and parent material all had significant interactions with fraction. Overall, fraction had more significant interactions with soil forming factors for C abundance than for C persistence.

The effect of MAT was modified by both fraction type and depth (fraction × depth × MAT, $F = 6.6$, $p = .001$; Figure 6). C abundance in the free particulate fraction of shallow soils showed the expected decrease with increasing MAT. In contrast, C abundance increased with MAT in the occluded particulate and mineral-associated fractions at all depths. The effect of wetness index was also modified by fraction and depth (fraction × depth × wetness index, $F = 5.9$, $p = .003$, Figure 7). C abundance in all fractions tended to increase as the wetness index increased, but the effect was stronger in the occluded particulate and mineral-associated fractions than in the free particulate fraction, and the effect was stronger in the surface soils for the free particulate and mineral-associated fractions (Figure 7 and S11). In the subsurface, increasing wetness index corresponded to increased C in the occluded particulate fraction, but led to no

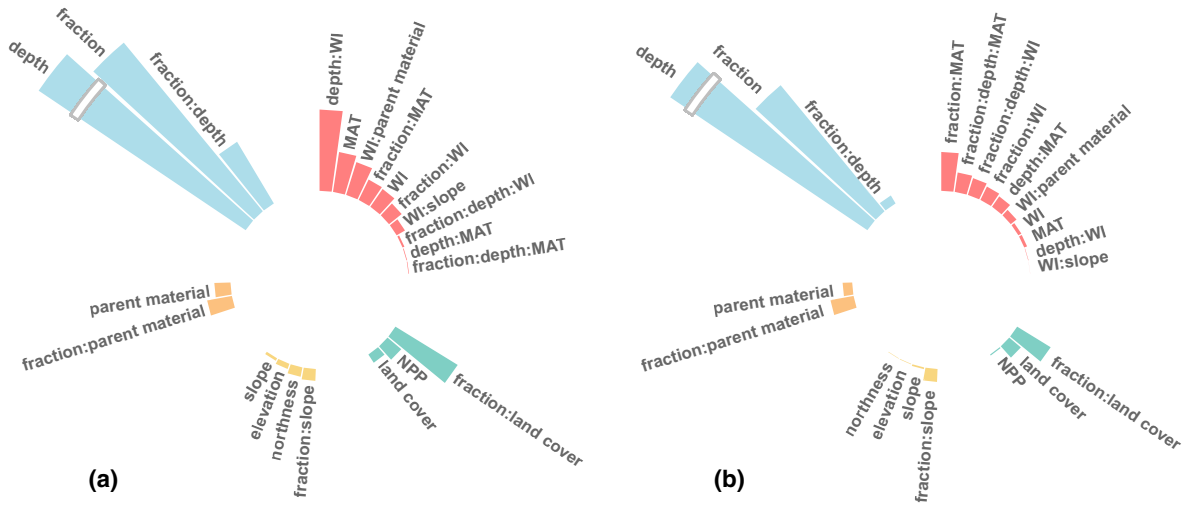

FIGURE 3 Size of bar indicates relative size of *F* values for fixed effects for (a) $\Delta^{14}C$, and (b) C mg g^{-1}. Effects are grouped according to soil forming factor. A break in the scale for the depth effect was implemented in (a) to allow for examination of the other effects which would not be highly visible due to the extremely high *F* value for the depth effect [Colour figure can be viewed at wileyonlinelibrary.com]

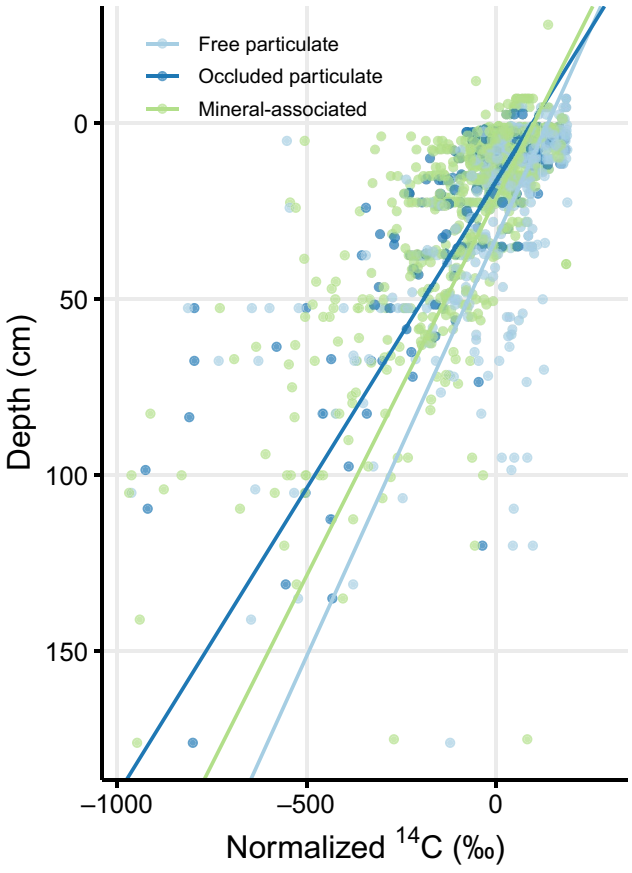

FIGURE 4 Normalized $\Delta^{14}C$ became more depleted with increasing soil depth indicating increased C persistence with depth. There was a significant depth × fraction interaction whereby C persistence increased more strongly with depth in the occluded particulate fraction and least strongly in the free particulate fraction. The lines show the predicted relationship for each fraction holding other continuous predictors at their means and with land cover and parent material factors set to "temperate forest" and "igneous intrusive" categories, respectively [Colour figure can be viewed at wileyonlinelibrary.com]

change in C within the free particulate and mineral-associated fractions. However, caution is warranted here because our dataset has no data on subsurface soils (>20 cm) from wetter ecosystems (wetness index > 1).

The influence of land cover varied by fraction type (fraction × land cover, $F = 13$, $p < .001$; Figure S8). Grasslands and croplands had the lowest C abundance in the free particulate fraction. Based on post hoc comparisons of marginal means, which were adjusted for the other effects in the model, grasslands had significantly less C in the free particulate fraction than temperate forests, tropical forests, and shrublands ($p < .027$). Croplands had significantly less free particulate C than shrublands ($p = .029$). For the occluded particulate fraction, boreal forests had less C than tropical forests, grasslands, and croplands ($p < .04$), and temperate forests had more C than grasslands and croplands ($p < .003$). Land cover was also a strong predictor of the proportion of C that was mineral associated ($F = 7$, $p = .0001$; Figure S6) with tropical forests, croplands, and grasslands having the largest proportions of mineral-associated C and temperate forests having the least (Figure 8).

Interactions among factors (including wetness index, relief, and parent material) explained smaller portions of variance. There was a significant interaction between fraction and slope for C abundance (fraction × slope, $F = 4.4$, $p = .013$; Figure S12); there was more mineral-associated C on steeper slopes. The relationships of the fractions to one another varied within parent material classes (fraction × parent material, $F = 7.9$, $p < .001$). For example, while the mineral fraction had more C than the free particulate fraction in most parent materials, in soils derived from igneous intrusive materials, fractions did not differ in C abundance ($p = .18$). Among parent materials, igneous intrusive had the lowest C abundance in the mineral fraction, while loess had the lowest C abundance in the free and occluded particulate fractions (Figure S10). The effect of parent material was additionally tied to the wetness index (wetness index × parent material, $F = 2.5$, $p < .041$). In igneous pyroclastic and

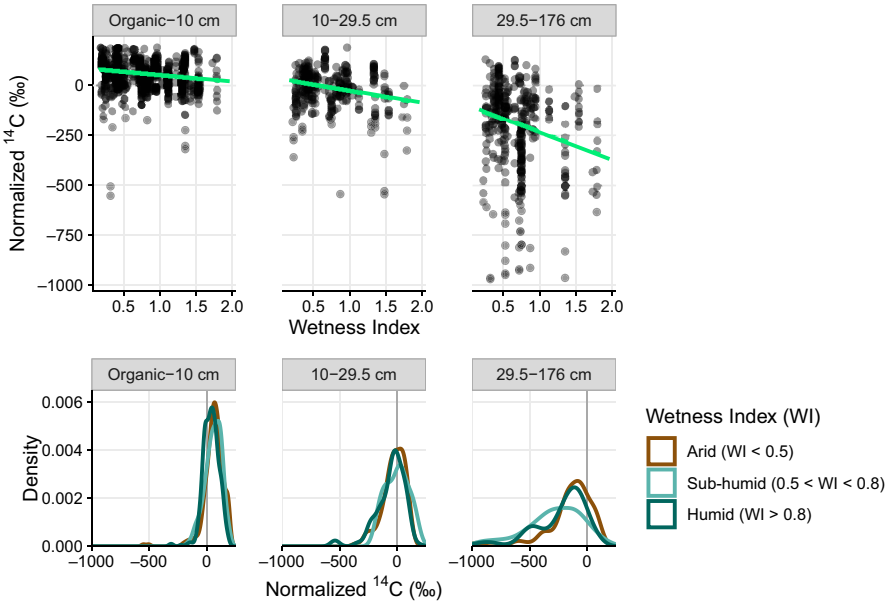

FIGURE 5 Normalized Δ^{14}C by wetness index grouped by depth interval (cm). The green lines show the predicted relationships holding other continuous predictors at their means and with land cover set to "temperate forest" and parent material set to "igneous intrusive." Each data point is a transparent grey, so the darker the shade, the more data in that area of the graph. Lower panel shows histograms of the data distribution for three wetness index categories binned by depth [Colour figure can be viewed at wileyonlinelibrary.com]

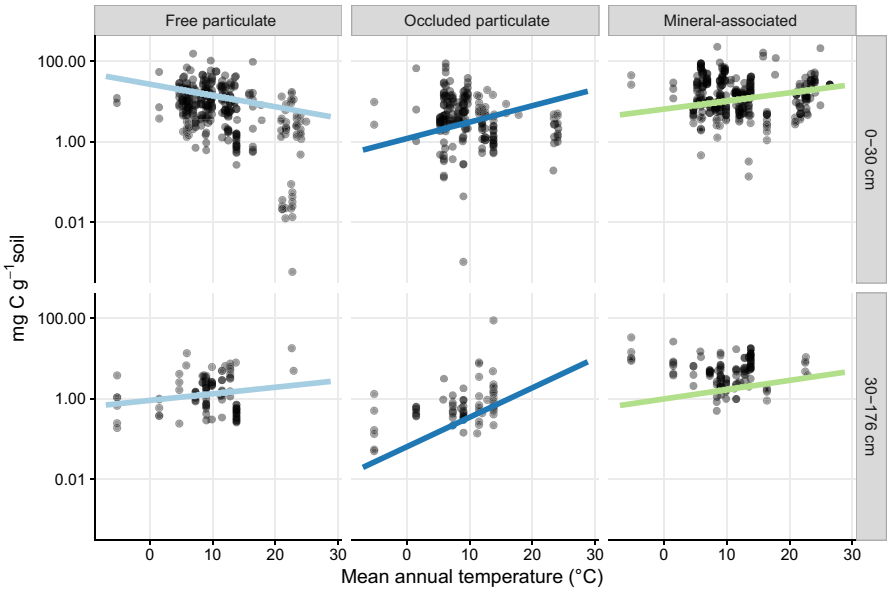

FIGURE 6 C abundance (mg C g^{-1} soil) versus mean annual temperature. The relationship varied both by depth and fraction. Data are binned by fraction type on the *x*-axis and depth interval on the *y*-axis. The lines show the predicted relationships holding other continuous predictors at their means and with land cover set to "temperate forest" and parent material set to "igneous intrusive" [Colour figure can be viewed at wileyonlinelibrary.com]

igneous extrusive parent materials, increasing wetness led to greater C abundance (Figure S10).

Across our models, the lack of significance observed for some factors is also important. For example, soil C abundance and persistence did not show a significant relationship NPP. Additionally, while sloped landscapes are well represented in the dataset (Figure S3), the predictor variables associated with relief (northness, slope, and elevation) were not significant in our models with the exception of the slope × wetness index interaction in the C abundance model. Finally, in this synthesis, soil parent material alone did not play a large role in explaining variation in soil C persistence and abundance or in the proportion of C associated with minerals at the global scale; however, it did significantly interact with wetness index in all models.

4 | DISCUSSION

The applied models explained over half the variation in C (mg C g^{-1} soil) and Δ^{14}C (‰) concentrations across the fractions. However, the relative influence of the various soil forming factors on C and Δ^{14}C concentrations differed, indicating that C abundance and persistence are regulated in distinct ways. These results offer an argument against confounding stock size with stock persistence in modelling efforts and further suggest that current soil C stock size alone may not be a good predictor of potential C losses associated with climate change, as some have argued (Van Gestel et al., 2018). This meta-analysis offers insight into more effective partitioning of C into conceptual pools with distinct Δ^{14}C values, which can be useful for model validation.

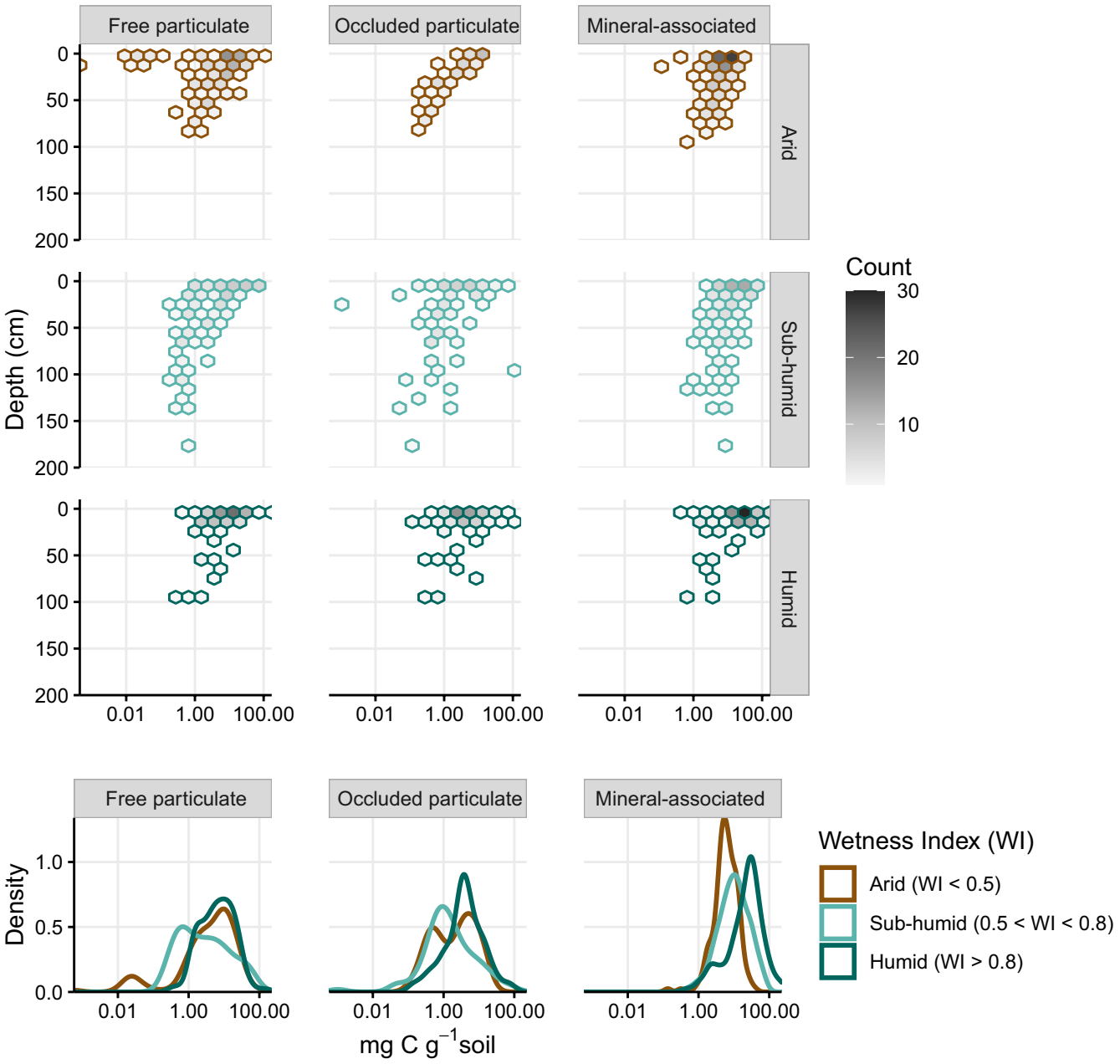

FIGURE 7 Normalized mg C per g of soil with depth, grouped by wetness index and fraction type. Each hexagon is a 2D bin (for each bin, $n = 15$). The darker the shade, the more data points are in the hexagon. Lower panel shows histograms of data distribution across all depths [Colour figure can be viewed at wileyonlinelibrary.com]

Soil depth was the single most important factor explaining variation in C abundance and persistence. Second to depth in explanatory power was fraction type, illustrating the heterogeneous nature of soil organic C, and supporting the partitioning of bulk soil organic C into fractions with different relationships to (de)stabilization mechanisms (Cotrufo et al., 2019; Lavallee et al., 2020). Climate significantly influenced both soil organic C abundance and persistence, though relationships varied by fraction and depth and the effects of temperature and moisture were different. The influence of specific soil forming factors is discussed in detail below using *F*-values from LMMs as a relative measure of the influence of each model parameter.

4.1 | Soil fraction

Globally, more C is stored in the mineral-associated fraction than in either of the particulate fractions, highlighting the important role of mineral protection in regulating C stocks. The relative enrichment of $\delta^{13}C$ and $\delta^{15}N$ and the lower C:N in the mineral-associated fraction is consistent with the interpretation that mineral-associated organic matter has undergone more microbial processing than particulate organic matter (Boström et al., 2007). Furthermore, lower $\Delta^{14}C$ (less enriched) values indicate that mineral-associated soil organic C is more persistent than either particulate soil organic C fraction. While the best way to separate bulk soil organic C into distinct fractions

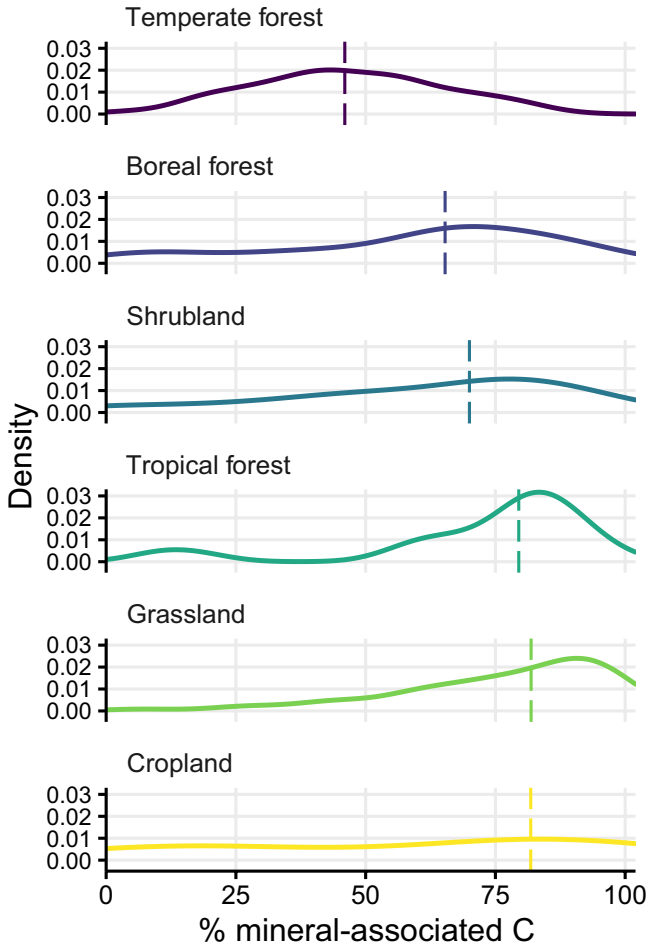

FIGURE 8 The percent of total soil C that is mineral-associated grouped by land cover. The lines indicate the median of the distribution [Colour figure can be viewed at wileyonlinelibrary.com]

with internally homogeneous characteristics and turnover rates is debated (Feng et al., 2016), the consistent differences across fractions in this global dataset suggest that it is reasonable to use density to separate bulk soil into meaningful pools that differ in their mechanisms of physicochemical protection. Individual studies have noted differences in the character of soil organic C and $\Delta^{14}C$ values of these three fractions (Golchin et al., 1994; Schrumpf et al., 2013; Swanston et al., 2005; Wagai et al., 2009), but until now it was unknown whether these patterns hold across the diversity of soils represented at the global scale.

4.2 | Depth

Soil depth was the property most strongly related to C abundance and persistence in soil density fractions, with abundance decreasing and persistence increasing with increasing depth, consistent with recent investigations into bulk C abundance (Rasmussen et al., 2018). In keeping with previous global-scale comparisons of mean age of surface (<30 cm) and subsurface (>30 cm) bulk soil organic C, we observed a significant and sharp decrease in soil $\Delta^{14}C$ values with depth in all fractions (Balesdent et al., 2018; He et al., 2016b; Shi et al., 2020), particularly in the protected occluded and mineral-associated fractions. Increasing microbial energy limitation and sorption capacity of soil minerals with depth, which both slow decomposition rates, are likely drivers of the depth effect (Ahrens et al., 2020). Also, we argue that depth represents the sum of weathering and transport processes over time, which contribute to a soil's maturity or development. In this view, depth is an integrative proxy, encapsulating a variety of processes and properties, including transport, moisture availability, reduced microbial access to substrate, and differences in soil mineral composition and morphology (e.g., illuvial horizons). This may explain why, although soil depth is strongly related to both C abundance and $\Delta^{14}C$, the relationship with $\Delta^{14}C$ is notably stronger. Both soil C abundance and radiocarbon are influenced by soil depth as the distance to the landscape surface influences the type and magnitude of modern C inputs to a particular soil horizon. However, $\Delta^{14}C$ is further coupled with depth as both properties evolve over timescales of centuries to millennia.

4.3 | Climate

Climate, manifested in models as changing temperature and precipitation, has long been assumed to be the primary determinant of soil organic C decomposition rates. However, the developing conceptual paradigm of soil organic C stabilization, which emphasizes chemical and physical protection, challenges this assumption (Lehmann et al., 2020; Miltner et al., 2011). Recent studies have found that soil chemical and mineral factors seem to have a greater influence on soil organic C persistence than climate factors (Doetterl et al., 2015; Mathieu et al., 2015). However, assessing the relative influence of soil chemical and mineral composition versus climate is complicated by the fact that they are inextricably linked. For instance, soil pH, and therefore the abundance of reactive metals and exchangeable cations, is directly affected by moisture availability (Slessarev et al., 2016).

Despite these recent challenges to the primacy of climate as the driver of soil C dynamics, we found that the climate variables, MAT, and wetness index (MAP/PET, a proxy for available moisture) were significant predictors of both $\Delta^{14}C$ and C abundance.

4.3.1 | Temperature

Decreasing C persistence in all fractions with increasing MAT is consistent with temperature's strong control over microbial activity (Liu et al., 2018). However, the expected decrease in C abundance with increasing MAT was only observed in the free particulate fraction of shallow soils (<30 cm). In contrast, C abundance increased with MAT in the occluded particulate and mineral-associated fractions at all depths. In the context of climate change, increases in temperature may thus decrease the amount of particulate organic C in surface layers, but may not substantially reduce aggregate- and mineral-associated C pools.

A recent meta-analysis of warming studies (Rocci et al., 2021) supports the assertion that increasing temperature will not reduce stabilized C pools—particulate C decreased more than mineral-associated C in response to warming. Sorption to mineral surfaces and occlusion within the small pores of soil aggregates protect C from microbial enzymatic attack and may render the associated C less sensitive to warming (Gentsch et al., 2018). While the free particulate fraction C is more microbially accessible than occluded particulate C, microbial decomposition in deeper soil horizons is often energy limited (Ahrens et al., 2020; Hicks Pries et al., 2018; Schimel, 2021), which may explain the attenuation of MAT's effect with depth. An increase in biological activity in response to temperature may actually promote C storage in the occluded and mineral-associated fractions. Enhanced plant, fungal, and soil fauna activities can promote soil aggregation (Soong & Nielsen, 2016; Tang et al., 2011), and enhanced decomposition can result in more microbial necromass becoming sorbed to mineral surfaces (Cotrufo et al., 2015).

In summary, higher temperatures were related to decreased persistence in all fractions. Despite that, higher temperatures are only associated with lower C storage for free particulate organics in the surface layers. In other fractions and deeper layers, the influence of warmer temperatures on C turnover is limited; thus, temperature-driven losses from occluded-particulate, mineral-associated, and subsurface pools may be less substantial under a warming climate. Although we cannot estimate the timescales required for soil fractions to re-equilibrate in response to temperature changes, we expect change will occur more quickly in response to temperature compared with other climate factors such as moisture, since changes in temperature are likely to result in accelerated microbial decomposition (e.g., Davidson & Janssens, 2006; Hicks Pries et al., 2017). This should be most apparent for the temperature-sensitive shallow particulate organic C fractions, which are also susceptible to indirect effects of temperature increases such as a greater prevalence of forest fires.

4.3.2 | Moisture

Wetness index was as strong of a predictor as MAT for both C abundance and persistence. And as with MAT, the relationship of soil C abundance to wetness index varied by fraction and depth. In general, soil C persistence was higher in humid ecosystems than in dry ecosystems, but the influence of wetness index on C persistence increased with increasing depth, indicating a stronger response to moisture in the subsurface.

Moisture availability can affect soil C through both production and stabilization processes that may have opposing effects on C persistence and abundance. First, greater moisture availability can lead to increased C inputs as plant productivity increases, which could explain why surface soil C abundance generally increases with increasing wetness index. Second, increased moisture has a nonlinear effect on decomposition, with rates typically increasing up to some threshold in moisture content (typically ~60% water-holding capacity), then decreasing at high moisture content (Greenwood, 1961; Keiluweit et al., 2018; Megonigal et al., 2004). In soils adapted to moisture fluctuations, however, high microbial activity can be maintained under both oxic and anoxic conditions (DeAngelis et al., 2010; Huang et al., 2021). Third, higher moisture levels can lead to greater transport of C to deeper soil layers. Finally, increased moisture may lead to greater soil throughflow that, over long time periods, increases soil weathering and depth through the development of the secondary clay, aluminum, and iron oxide minerals that are essential for protecting soil C (Rasmussen et al., 2018). This tension between C stabilization versus decomposition is especially evident for iron-mineral-associated C. Short periods of high moisture generate reduced iron [Fe(II)] that can oxidize and form strong Fe(III) mineral-organic co-precipitates that contribute to C persistence. However, unless these iron-C associations are protected via subsequent occlusion or surface coating, they are likely vulnerable to dissolution if high moisture conditions resume (Chen et al., 2020). Another tension is that increased transport of dissolved organic C could lead to either less or more C at depth depending on whether those simple C molecules stimulate microbial decomposition ("priming"; Luo et al., 2020) or form mineral associations. The less positive response of C abundance to moisture in the free particulate fraction at depth (Figure S11) may reflect the priming effect. In the mineral-associated fraction, the sorption capacity of minerals could drive the effect of moisture on soil C persistence. Increasing moisture could therefore lead to accumulation of more persistent (more depleted $\Delta^{14}C$) C at depth (Ahrens et al., 2020), which is indeed what we found in our analysis.

The relative strength of these different moisture-driven mechanisms on various soil fractions, depths, and parent materials will determine the timescales and overall response of soil C to changes in soil moisture. For example, if C persistence is driven primarily by the influence of soil moisture on weathering, which integrates the effect of increased moisture over geologic time, we might not see an effect on C persistence in this century. Meanwhile, if the effects of changing moisture on C abundance are driven by inputs, we might predict that areas expected to become hotter and drier will have decreased C in the surface as inputs slow but a buildup of C in the subsurface as priming ceases. The significant interactions of wetness index with depth and fraction type, as well the complexity of the mechanisms through which it can act on soil C highlights the need for empirical research into the effects of changing moisture on soil C and its interaction with other variables such as temperature. These interactions additionally point to the importance of developing reactive transport models that can capture how moisture interacts with both soil C and minerals (Hénin & Dupuis, 1945; Rasmussen et al., 2018; Shi et al., 2020) and the utility of considering climate drivers in the context of soil functional heterogeneity (e.g., soil fractions). Previous investigations using bulk $\Delta^{14}C$ may have failed to find significant relationships among bulk C stocks and bulk $\Delta^{14}C$ and climate (Doetterl et al., 2015; Mathieu et al., 2015) because the whole soil response is the summation of the responses of its fractions, which can have opposing relationships with climate factors. The fact that

the fractions exhibited different relationships to climate variables strongly suggests that partitioning bulk soil organic C into pools based on protection mechanisms is integral to understanding and predicting its response to climate change (Rocci et al., 2021).

4.4 | Organisms (vegetation)

Soil C abundance and persistence within different fractions varied among land cover types, with the influence of vegetation seemingly stronger for particulate fractions than mineral-associated C. Despite tropical forests having the highest amount of mineral-associated C, there were no significant differences in the abundance of mineral-associated C among land cover types (Figure S8). Given that particulate fractions are generally less decomposed, and thus closer chemically and structurally to the original plant litter inputs, it makes sense that the effect of vegetation on C abundance was most important for the free and occluded fractions. For example, lower particulate C abundance in grasslands and croplands relative to forests and shrublands are likely due to the lack of slow-to-decompose woody litter inputs. The unique relationships of fraction C abundance and persistence within land cover types again emphasize the need to examine soil fractions in addition to bulk soil trends.

Carbon persistence generally varied ($\Delta^{14}C$) among fractions within a land cover type, with persistence generally greater in mineral-associated fractions. However, there was a large amount of variation in the relative abundance and persistence of the fractions across land cover types. These interactions suggest that vegetation controls the relative strength of stabilization mechanisms (e.g., aggregation vs. mineral sorption) within a soil as well as influencing the partitioning of C between mineral-associated and particulate fractions. Additionally, we observed that croplands had the least persistent occluded particulate fraction C of all land covers, consistent with tillage effects that disrupt aggregates and lessen their ability to protect C from microbes (Six et al., 1998).

Surprisingly, soil C abundance and persistence did not show a significant relationship with NPP. The lack of a relationship between C abundance and NPP may be the result of covariance among NPP and climate variables, particularly the wetness index, which was significantly correlated with NPP (Pearson's $r = 0.52$). For example, tropical forests had the highest abundance of mineral-associated C, but not significantly so, because the high abundance was likely explained by warmer temperatures leading to more rapid decomposition of litter inputs and greater moisture availability leading to more highly weathered soils (Marin-Spiotta et al., 2009).

4.5 | Relief

Predictor variables associated with relief (northness, slope, and elevation) were not strongly significant in our models. Numerous studies have illustrated strong variability of soil characteristics such as depth, C abundance, and $\Delta^{14}C$ associated with different hillslope positions and aspects (Berhe et al., 2012; Hall et al., 2015); however, the influence of relief is muddled at the global scale and may be partly explained by our strong depth predictor. We observed a greater abundance of mineral-associated C on steeper slopes, which warrants further investigation. The influence of relief or topography on soils is manifest through local scale variations in soil conditions including temperature, moisture, depth, vegetation, and soil structure. Therefore, at the global scale, it is unsurprising that parameters other than relief better explained the observed variability.

4.6 | Parent material

Given the importance of mineral composition in driving C abundance (Rasmussen et al., 2018) and persistence (e.g., Heckman et al., 2018; Porras et al., 2017; Torn et al., 1997) across scales and regions, we expected that parent material would have a large influence on C abundance and persistence. Previous work has inferred a strong influence of soil parent material on the abundance and persistence of C (Reichenbach et al., 2021), with igneous extrusive and pyroclastic lithologies (volcanic ash and lava flows) often associated with extraordinarily high soil C concentrations and abundances (Egli et al., 2008; Marin-Spiotta et al., 2011). In this synthesis, soil parent material alone does not appear to play a significant role in explaining variation in soil C persistence and abundance at the global scale. However, mineral composition is a function of soil development, so that even among soils derived from igneous parent materials, there is a great deal of variation in the amount of short-range order minerals with high sorptive capacities driven by age, temperature, and moisture (Lawrence et al., 2015; Rasmussen et al., 2018; Torn et al., 1997; Von Fromm et al., 2021). Logically, as moisture increases, weathering and sorptive surface area also increase, leading to the greater protection of C on reactive secondary mineral surfaces. Consistent with these weathering processes, soils developed from igneous extrusive, igneous pyroclastic, and sedimentary-clastic parent materials increased in C persistence with increasing moisture across the sampled range of wetness index values (0.25–1.75). In igneous pyroclastic and igneous extrusive parent materials, increasing wetness also led to greater C abundance. However, certain parent materials, like loess, had the opposite relationship with wetness index, though the range of wetness index values in loess only included drier sites (0.2–0.9).

4.7 | Unexplained variance

Forty percent of the variance in soil C abundance and $\Delta^{14}C$ remained unexplained by our linear mixed-effect models after accounting for the influence of soil forming factors, depth,

and fraction type on C abundance and persistence. Our analysis focused on using soil forming factors that encapsulate environmental constraints external to, and independent of, the soil itself to predict soil C abundance and persistence; much of the unexplained variance may well be described by soil properties that evolve in response to the soil forming factors, namely soil physicochemical properties such as the reactivity of metals and minerals or microbial community composition and function. Soils are complex systems with myriad feedbacks and interdependence among biotic and abiotic components (Schimel, 2021) that are difficult to assess with existing datasets. The analysis presented here, however, highlights future opportunities and data gaps for expanding our ability to model soil C variability. For example, more information regarding the distribution of C inputs, microbial community composition and function, land-use history, or degree of soil development would likely account for this unexplained variance. Additionally, though the current dataset does a good job matching the global variation of soils in major climate and relief factors, it does not allow for assessment of variation at finer spatial scales.

Better quantification of soil organic C inputs is essential to further constrain partitioning of C between soil pools. For instance, the MODIS-derived NPP data used in these analyses do not reflect the partitioning of productivity between above- and belowground tissues, which may be important because belowground inputs are retained in soil organic C at a higher rate than aboveground inputs (Jackson et al., 2017). At present, belowground NPP, root density, and root biomass metrics are not well quantified at large spatial scales. Furthermore, increasing our understanding of soil organic C origin (e.g., root vs. shoot) and composition (Hall et al., 2020) should increase our understanding of the role of C inputs in regulating turnover (Poeplau et al., 2021).

Microbial community composition and functional traits may also contribute substantially to observed variance in C abundance and persistence. Differences in C cycling have been associated with arbuscular mycorrhizal versus ectomycorrhizal systems (Craig et al., 2019), as well as differences in fungal to bacterial ratios in the soil (Malik et al., 2016). Yet, large-scale quantification of the influence of soil microbial communities, which directly drive soil C turnover and formation of stable C pools, is difficult to assess given the complexity of tools such as advanced genetic techniques (e.g., metabolomics and proteomics). High-throughput phospholipid fatty acid (PLFA) analysis (Ellis & Ritz, 2018) may offer the opportunity to represent variance associated with community composition and biomass at scales meaningful for ecosystem or global modelers, because PLFAs are more robustly quantitative for total bacteria than are current 'omics methods. Databases such as FungalRoot (Soudzilovskaia et al., 2020) and the Global Soil Biodiversity Initiative may also offer a way forward.

Approximately a third of global soils are considered degraded by some form of anthropogenic disturbance, with most arable land being manipulated in some way (Shukla et al., 2019). Of the global ice-free surface, 12% of soils are utilized for crop production, 37% for pasture, and 22% for plantation forests (Shukla et al., 2019). However, our study has revealed a strong researcher bias to apply density fractionation, in combination with radiocarbon measurement, in unmanaged or minimally managed temperate forest systems, despite evidence that land-use activities can alter distribution and persistence of C among fractions (Sanderman et al., 2017; Sulman et al., 2020). In our study, cropland had a relatively low abundance of particulate fraction and was the only land cover where the occluded fraction was less persistent than the free light fraction, potentially due to aggregate disruption by tillage or erosional loss of particulate C. Given the drastic losses and redistribution of C associated with cropping (Sanderman et al., 2017), if future more work were to examine density fractionation in managed soils, the influence and legacy of disturbance on soil organic C cycling could be assessed (Sulman et al., 2020).

4.8 | Time

Time is the one soil forming factor that was notably absent from our analysis. Time does not, on its own, directly control soil C cycling. Rather, time measures the duration that the soil has been affected by other soil forming factors. Soil properties evolve and change over time, and the trajectory of soil properties is a function of internal feedbacks and deterministic and stochastic processes that may be somewhat disconnected from external forcings. The change in soil properties over time may not consistently favor the development of physiochemical conditions that increase C persistence and abundance. Therefore, internal soil properties themselves (i.e., mineral composition, profile depth) may best capture time in predicting soil C. Indeed, soil chronosequence studies demonstrate that soil physicochemical properties such as pH, short-range order minerals, or particle-specific surface area are better predictors of $\Delta^{14}C$ than are climate variables directly (Lawrence et al., 2015; Masiello et al., 2004; Torn et al., 1997).

In lieu of soil age, we tested soil order as an integrative proxy for soil development, since with increasing time, soils develop unique physicochemical properties (Mathieu et al., 2015; Schaetzl & Anderson, 2005). To test if a soil forming factor we had not considered could account for unexplained variance, we regressed our model residuals against soil order. Soil order did not explain any meaningful additional model variation implying we had explained all the variance we could with traditional soil forming factors. We additionally explored how C partitioning to the heavy fraction might vary by soil forming factor, but this model yielded few additional insights beyond the importance of land cover.

Quantifying the timescales and efficiencies for which C inputs are converted to various forms of soil organic carbon (SOC), including particulate and mineral-associated pools, aids in understanding the heterogeneity of C ages within measured or modeled pools and for developing strategies for increasing SOC sequestration. In a recent synthesis, Villarino et al. (2021) suggested the formation of mineral-associated C occurs rapidly following inputs

with formation efficiencies between 7% and 46%, dependent on the source of C input (e.g., aboveground litter, roots, or rhizodeposition). Such results are difficult to square with radiocarbon-based age estimates, particularly for mineral-associated C pools with long and variable radiocarbon-based mean ages (mean age of 6255 years with a standard error of 1812 years and a median age of 396 years). This discrepancy highlights the potential heterogeneity within a given C pool and implies a transient nature of recently formed SOC pools. Distributions of soil C ages within a pool can have very long tails, so that a small amount of very old C can skew the mean age older than the majority of the C in the pool (Sierra et al., 2018). More work is required to link the accretion of SOC observed in short-term field and laboratory studies with the long-term persistence of SOC pools suggested from radiocarbon-based fractionation studies and to understand how various factors of soil formation may couple SOC preservation across these different temporal scales.

4.9 | Integrated framework for interpreting these results

We chose to examine soil C fraction dynamics within the context of the soil forming factors because these basic factors are acknowledged as important controls on soil properties. Of the "CLORPT" factors, climate, organisms, and parent material emerge from our analysis as consistently influencing the distribution and age of soil organic C. Depth and fraction type explained the most variance, overwhelmingly so in the case of persistence. Climate variables were important predictors of both C abundance and persistence. Although climate variables have long been regarded as important controls on the balance between soil C inputs and losses, our analyses of soil fraction data reinforce a more nuanced view of the mechanisms through which climate may influence soil C cycling. Specifically, the influence of climate on the C dynamics of the free particulate fraction is driven by the effect of temperature on microbial metabolism, whereas the influence of climate on the mineral fraction is likely linked to long-term climate-driven controls on the composition and distribution of secondary minerals through soil weathering.

The processes through which climate factors influence soil C cycling may reflect the competing influence of reaction rates versus transport rates. For example, increasing temperature drives higher rates of cycling, including greater input and output fluxes (Giardina et al., 2014). The net result is depleted $\Delta^{14}C$ values (i.e., longer turnover times) in cooler soils versus enriched $\Delta^{14}C$ in warmer soils (i.e., shorter turnover times). In contrast, moisture drives formation and transport of solutes, and through time, differences in transport rates can lead to different patterns of secondary mineral formation (e.g., Lawrence et al., 2015). Since transport occurs predominantly downward, it is common to observe a significant interaction of wetness index and depth (Figures 2 and 5). The link between available moisture, transport, and weathering is especially evident in the strong variation in mineral-associated C abundance according to wetness index (Figure 7). Our findings suggest that process-based models are well suited to highlighting the interplay between soil organic C reactivity and transport necessary for projecting future soil organic C responses.

Overall, the most meaningful result is the importance of fraction type. Fractions significantly differed from one another in abundance and chemistry (Table 2). Fraction type was second to depth in explaining variation in both C abundance and persistence and had many significant interactions with soil forming factors. Fractions responded differently to temperature and moisture indicating they vary in their vulnerability to climate change. The fractions are differently affected by vegetation as shown by the influence of land cover type on the amount of C in the particulate fractions and also on the partitioning of C among fractions. Fraction data on soil organic C and $\Delta^{14}C$ are therefore valuable for developing and testing global scale models—they capture the heterogeneity of the amount and persistence of C within soils.

ACKNOWLEDGMENTS

Essential support for this project came from the U.S. Geological Survey (USGS) John Wesley Powell Center for Analysis and Synthesis Working Group on Soil Carbon: "What lies below? Improving quantification and prediction of soil carbon storage, stability, and susceptibility to disturbance." Additional funding was provided by the Max Planck Institute for Biogeochemistry, the European Research Council (Horizon 2020 Research and Innovation Programme, grant agreement 695101), the USGS Land Change Science mission area, and the US Department of Agriculture (Soil Carbon Working Group award 2018-67003-27935). We specifically acknowledge the intellectual and financial contributions of Dr. Susan Trumbore of the Max Planck Institute for Biogeochemistry. Any use of trade, firm, or product names is for descriptive purposes only and does not imply endorsement by the U.S. Government.

CONFLICT OF INTEREST

The authors declare no conflict of interest.

DATA AVAILABILITY STATEMENT

The data that support the findings of this study are available in the supplementary material of this article and online at https://doi.org/10.5281/zenodo.5736535.

ORCID

Katherine Heckman https://orcid.org/0000-0003-2265-4542
Susan E. Crow https://orcid.org/0000-0001-8735-1580
Alison M. Hoyt https://orcid.org/0000-0003-0813-5084
Sophie F. von Fromm https://orcid.org/0000-0002-1820-1455
Casey McGrath https://orcid.org/0000-0002-8808-8312
Alain F. Plante https://orcid.org/0000-0003-0124-6187
Carlos A. Sierra https://orcid.org/0000-0003-0009-4169
Rota Wagai https://orcid.org/0000-0003-3890-8025

REFERENCES

Ågren, G. I., Bosatta, E., & Agren, G. I. (1996). Quality: A bridge between theory and experiment in soil organic matter studies. *Oikos*, *76*(3), 522–528. https://doi.org/10.2307/3546345

Ahrens, B., Guggenberger, G., Rethemeyer, J., John, S., Marschner, B., Heinze, S., Angst, G., Mueller, C. W., Kögel-Knabner, I., Leuschner, C., Hertel, D., Bachmann, J., Reichstein, M., & Schrumpf, M. (2020). Combination of energy limitation and sorption capacity explains ^{14}C depth gradients. *Soil Biology and Biochemistry*, *148*, 107912. https://doi.org/10.1016/j.soilbio.2020.107912

Baisden, W., Amundson, R., Cook, A., & Brenner, D. (2002). Turnover and storage of C and N in five density fractions from California annual grassland surface soils. *Global Biogeochemical Cycles*, *16*, 64-1–64-16. https://doi.org/10.1029/2001GB001822

Baisden, W., & Canessa, S. (2013). Using 50 years of soil radiocarbon data to identify optimal approaches for estimating soil carbon residence times. *Nuclear Instruments and Methods in Physics Research Section B: Beam Interactions with Materials and Atoms*, *294*, 588–592. https://doi.org/10.1016/j.nimb.2012.06.021

Balesdent, J., Basile-Doelsch, I., Chadoeuf, J., Cornu, S., Derrien, D., Fekiacova, Z., & Hatté, C. (2018). Atmosphere–soil carbon transfer as a function of soil depth. *Nature*, *559*, 599–602. https://doi.org/10.1038/s41586-018-0328-3

Bartoń, K. (2019). *MuMIn: Multi-modal inference. Model selection and model averaging based on information criteria (AICc and alike)*. R package version 1.4.3. (6th ed.).

Bates, D., Mächler, M., Bolker, B., & Walker, S. (2014). *Fitting linear mixed-effects models using lme4*. arXiv.org.preprint.

Beem-Miller, J., Monroe, J. G., Hoyt, A. M., Stoner, S., von Fromm, S., Lawrence, C. R., & Sierra, C. A. (2021). ISRaD (Version 1.7.8) [Computer software]. https://github.com/International-Soil-Radiocarbon-Database/ISRaD/

Berhe, A. A., Harden, J. W., Torn, M. S., Kleber, M., Burton, S. D., & Harte, J. (2012). Persistence of soil organic matter in eroding versus depositional landform positions. *Journal of Geophysical Research: Biogeosciences*, 117. https://doi.org/10.1029/2011JG001790

Blankinship, J. C., Berhe, A. A., Crow, S. E., Druhan, J. L., Heckman, K. A., Keiluweit, M., Lawrence, C. R., Marín-Spiotta, E., Plante, A. F., Rasmussen, C., Schädel, C., Schimel, J. P., Sierra, C. A., Thompson, A., Wagai, R., & Wieder, W. R. (2018). Improving understanding of soil organic matter dynamics by triangulating theories, measurements, and models. *Biogeochemistry*, *140*, 1–13. https://doi.org/10.1007/s10533-018-0478-2

Bongiorno, G., Bünemann, E. K., Oguejiofor, C. U., Meier, J., Gort, G., Comans, R., Mäder, P., Brussaard, L., & de Goede, R. (2019). Sensitivity of labile carbon fractions to tillage and organic matter management and their potential as comprehensive soil quality indicators across pedoclimatic conditions in Europe. *Ecological Indicators*, *99*, 38–50. https://doi.org/10.1016/j.ecolind.2018.12.008

Boström, B., Comstedt, D., & Ekblad, A. (2007). Isotope fractionation and ^{13}C enrichment in soil profiles during the decomposition of soil organic matter. *Oecologia*, *153*, 89–98. https://doi.org/10.1007/s00442-007-0700-8

Bradford, M. A., Wieder, W. R., Bonan, G. B., Fierer, N., Raymond, P. A., & Crowther, T. W. (2016). Managing uncertainty in soil carbon feedbacks to climate change. *Nature Climate Change*, *6*, 751–758. https://doi.org/10.1038/nclimate3071

Buchkowski, R. W., Shaw, A. N., Sihi, D., Smith, G. R., & Keiser, A. D. (2019). Constraining carbon and nutrient flows in soil with ecological stoichiometry. *Frontiers in Ecology and Evolution*, *7*, 382. https://doi.org/10.3389/fevo.2019.00382

Carpenter, S. R. (1981). Decay of heterogenous detritus: A general model. *Journal of Theoretical Biology*, *89*, 539–547. https://doi.org/10.1016/0022-5193(81)90026-6

Chen, C., Hall, S. J., Coward, E., & Thompson, A. (2020). Iron-mediated organic matter decomposition in humid soils can counteract protection. *Nature Communications*, *11*, 1–13. https://doi.org/10.1038/s41467-020-16071-5

Cotrufo, M. F., Ranalli, M. G., Haddix, M. L., Six, J., & Lugato, E. (2019). Soil carbon storage informed by particulate and mineral-associated organic matter. *Nature Geoscience*, *12*, 989–994. https://doi.org/10.1038/s41561-019-0484-6

Cotrufo, M. F., Soong, J. L., Horton, A. J., Campbell, E. E., Haddix, M. L., Wall, D. H., & Parton, W. J. (2015). Formation of soil organic matter via biochemical and physical pathways of litter mass loss. *Nature Geoscience*, *8*, 776–779. https://doi.org/10.1038/ngeo2520

Cotrufo, M. F., Wallenstein, M. D., Boot, C. M., Denef, K., & Paul, E. (2013). The Microbial Efficiency-Matrix Stabilization (MEMS) framework integrates plant litter decomposition with soil organic matter stabilization: Do labile plant inputs form stable soil organic matter? *Global Change Biology*, *19*, 988–995. https://doi.org/10.1111/gcb.12113

Craig, M. E., Lovko, N., Flory, S. L., Wright, J. P., & Phillips, R. P. (2019). Impacts of an invasive grass on soil organic matter pools vary across a tree-mycorrhizal gradient. *Biogeochemistry*, *144*, 149–164. https://doi.org/10.1007/s10533-019-00577-2

Crow, S. E., & Sierra, C. A. (2018). Dynamic, intermediate soil carbon pools may drive future responsiveness to environmental change. *Journal of Environmental Quality*, *47*, 607–616. https://doi.org/10.2134/jeq2017.07.0280

Davidson, E. A., & Janssens, I. A. (2006). Temperature sensitivity of soil carbon decomposition and feedbacks to climate change. *Nature*, *440*, 165–173. https://doi.org/10.1038/nature04514

DeAngelis, K. M., Silver, W. L., Thompson, A. W., & Firestone, M. K. (2010). Microbial communities acclimate to recurring changes in soil redox potential status. *Environmental Microbiology*, *12*, 3137–3149. https://doi.org/10.1111/j.1462-2920.2010.02286.x

Doetterl, S., Stevens, A., Six, J., Merckx, R., Van Oost, K., Casanova Pinto, M., Casanova-Katny, A., Muñoz, C., Boudin, M., Zagal Venegas, E., & Boeckx, P. (2015). Soil carbon storage controlled by interactions between geochemistry and climate. *Nature Geoscience*, *8*, 780–783. https://doi.org/10.1038/ngeo2516

Dokuchaev, V. (1883). Russian Chernozem. Report to the Imperial Free Economic Society (Tipogr. Declerona i Evdokimova), St. Petersburg, Russia.

Dormann, C. F., Elith, J., Bacher, S., Buchmann, C., Carl, G., Carré, G., Marquéz, J. R. G., Gruber, B., Lafourcade, B., Leitão, P. J., Münkemüller, T., McClean, C., Osborne, P. E., Reineking, B., Schröder, B., Skidmore, A. K., Zurell, D., & Lautenbach, S. (2013). Collinearity: A review of methods to deal with it and a simulation study evaluating their performance. *Ecography*, *36*, 27–46. https://doi.org/10.1111/j.1600-0587.2012.07348.x

Egli, M., Nater, M., Mirabella, A., Raimondi, S., Plötze, M., & Alioth, L. (2008). Clay minerals, oxyhydroxide formation, element leaching and humus development in volcanic soils. *Geoderma*, *143*, 101–114. https://doi.org/10.1016/j.geoderma.2007.10.020

Elliott, E. T., Paustian, K., & Frey, S. D. (1996). Modeling the measurable or measuring the modelable: A hierarchical approach to isolating meaningful soil organic matter fractionations. In D. S. Powlson, P. Smith, & J. U. Smith (Eds.), *Evaluation of soil organic matter models* (pp. 161–179). Springer.

Ellis, S., & Ritz, K. (2018). A modified high-throughput analysis of PLFAs in soil. *MethodsX*, *5*, 1491–1497. https://doi.org/10.1016/j.mex.2018.10.022

Feng, W., Shi, Z., Jiang, J., Xia, J., Liang, J., Zhou, J., & Luo, Y. (2016). Methodological uncertainty in estimating carbon turnover times of soil fractions. *Soil Biology and Biochemistry*, *100*, 118–124. https://doi.org/10.1016/j.soilbio.2016.06.003

Friedlingstein, P., Meinshausen, M., Arora, V. K., Jones, C. D., Anav, A., Liddicoat, S. K., & Knutti, R. (2014). Uncertainties in CMIP5 climate

projections due to carbon cycle feedbacks. *Journal of Climate*, *27*, 511–526. https://doi.org/10.1175/JCLI-D-12-00579.1

Gaudinski, J. B., Trumbore, S. E., Davidson, E. A., & Zheng, S. (2000). Soil carbon cycling in a temperate forest: Radiocarbon-based estimates of residence times, sequestration rates and partitioning of fluxes. *Biogeochemistry*, *51*, 33–69.

Gentsch, N., Wild, B., Mikutta, R., Čapek, P., Diáková, K., Schrumpf, M., Turner, S., Minnich, C., Schaarschmidt, F., Shibistova, O., Schnecker, J., Urich, T., Gittel, A., Šantrůčková, H., Bárta, J., Lashchinskiy, N., Fuß, R., Richter, A., & Guggenberger, G. (2018). Temperature response of permafrost soil carbon is attenuated by mineral protection. *Global Change Biology*, *24*, 3401–3415. https://doi.org/10.1111/gcb.14316

Giardina, C. P., Litton, C. M., Crow, S. E., & Asner, G. P. (2014). Warming-related increases in soil CO_2 efflux are explained by increased below-ground carbon flux. *Nature Climate Change*, *4*, 822–827. https://doi.org/10.1038/nclimate2322

Golchin, A., Oades, J., Skjemstad, J., & Clarke, P. (1994). Study of free and occluded particulate organic matter in soils by solid state ^{13}C CP/MAS NMR spectroscopy and scanning electron microscopy. *Soil Research*, *32*, 285–309. https://doi.org/10.1071/SR9940285

Greenland, D. (1964). Separation of partially humified organic materials by ultrasonic dispersion. *Transactions Eighth International Congress of Soil Science*, *3*, 137–148.

Greenwood, D. (1961). The effect of oxygen concentration on the decomposition of organic materials in soil. *Plant and Soil*, *14*(4), 360–376. https://doi.org/10.1007/BF01666294

Hall, S. J., McNicol, G., Natake, T., & Silver, W. L. (2015). Large fluxes and rapid turnover of mineral-associated carbon across topographic gradients in a humid tropical forest: Insights from paired ^{14}C analysis. *Biogeosciences*, *12*, 2471–2487.

Hall, S. J., Ye, C., Weintraub, S. R., & Hockaday, W. C. (2020). Molecular trade-offs in soil organic carbon composition at continental scale. *Nature Geoscience*, *13*, 687–692. https://doi.org/10.1038/s41561-020-0634-x

He, Y., Trumbore, S. E., Torn, M. S., Harden, J. W., Vaughn, L. J., Allison, S. D., & Randerson, J. T. (2016a). Radiocarbon constraints imply reduced carbon uptake by soils during the 21st century. *Science*, *353*, 7. https://doi.org/10.1126/science.aad4273

He, Y., Trumbore, S. E., Torn, M. S., Harden, J. W., Vaughn, L. J., Allison, S. D., & Randerson, J. T. (2016b). Radiocarbon constraints imply reduced carbon uptake by soils during the 21st century. *Science*, *353*, 1419–1424. https://doi.org/10.1126/science.aad4273

Heckman, K., Throckmorton, H., Clingensmith, C., González Vila, F. J., Horwath, W. R., Knicker, H., & Rasmussen, C. (2014). Factors affecting the molecular structure and mean residence time of occluded organics in a lithosequence of soils under ponderosa pine. *Soil Biology and Biochemistry*, *77*, 1–11. https://doi.org/10.1016/j.soilbio.2014.05.028

Heckman, K., Throckmorton, H., Horwath, W., Swanston, C., & Rasmussen, C. (2018). Variation in the molecular structure and radiocarbon abundance of mineral-associated organic matter across a lithosequence of forest soils. *Soil Systems*, *2*. https://doi.org/10.3390/soilsystems2020036

Hénin, S., & Dupuis, M. (1945). *Essai de bilan de la matière organique du sol*. Dudod.

Hicks Pries, C. E., Castanha, C., Porras, R., & Torn, M. S. (2017). The whole-soil carbon flux in response to warming. *Science*, *355*(6332), 1420–1423. https://doi.org/10.1126/science.aal1319

Hicks Pries, C. E., Sulman, B. N., West, C., O'Neill, C., Poppleton, E., Porras, R. C., Castanha, C., Zhu, B., Wiedemeier, D. B., & Torn, M. S. (2018). Root litter decomposition slows with soil depth. *Soil Biology and Biochemistry*, *125*, 103–114. https://doi.org/10.1016/j.soilbio.2018.07.002

Hua, Q., Barbetti, M., & Rakowski, A. Z. (2013). Atmospheric radiocarbon for the period 1950–2010. *Radiocarbon*, *55*, 2059–2072. https://doi.org/10.2458/azu_js_rc.v55i2.16177

Huang, W., Wang, K., Ye, C., Hockaday, W. C., Wang, G., & Hall, S. J. (2021). High carbon losses from oxygen-limited soils challenge biogeochemical theory and model assumptions. *Global Change Biology*. https://doi.org/10.1111/gcb.15867

Jackson, R. B., Lajtha, K., Crow, S. E., Hugelius, G., Kramer, M. G., & Piñeiro, G. (2017). The ecology of soil carbon: Pools, vulnerabilities, and biotic and abiotic controls. *Annual Review of Ecology, Evolution, and Systematics*, *48*, 419–445. https://doi.org/10.1146/annurev-ecolsys-112414-054234

Jastrow, J., Miller, R., & Boutton, T. (1996). Carbon dynamics of aggregate-associated organic matter estimated by carbon-13 natural abundance. *Soil Science Society of America Journal*, *60*, 801–807. https://doi.org/10.2136/sssaj1996.03615995006000030017x

Jenny, H. (1941). *Factors of soil formation a system of quantitative pedology*. Dover Publications Inc.

Keiluweit, M., Gee, K., Denney, A., & Fendorf, S. (2018). Anoxic microsites in upland soils dominantly controlled by clay content. *Soil Biology and Biochemistry*, *118*, 42–50. https://doi.org/10.1016/j.soilbio.2017.12.002

Knorr, W., Prentice, I. C., House, J. I., & Holland, E. A. (2005). Long-term sensitivity of soil carbon turnover to warming. *Nature*, *433*(7023), 298–301.

Kuznetsova, A., Brockhoff, P., & Christensen, R. (2016). *Tests in linear mixed effects models version*. CRAN. Retrieved from https://cran.r-project.org/web/packages/lmerTest/lmerTest.pdf

Lavallee, J. M., Soong, J. L., & Cotrufo, M. F. (2020). Conceptualizing soil organic matter into particulate and mineral-associated forms to address global change in the 21st century. *Global Change Biology*, *26*, 261–273. https://doi.org/10.1111/gcb.14859

Lawrence, C. R., Beem-Miller, J., Hoyt, A. M., Monroe, G., Sierra, C. A., Stoner, S., Heckman, K., Blankinship, J. C., Crow, S. E., & McNicol, G. (2020). An open-source database for the synthesis of soil radiocarbon data: International Soil Radiocarbon Database (ISRaD) version 1.0. *Earth System Science Data*, *12*(1), 61–76.

Lawrence, C. R., Harden, J. W., Xu, X., Schulz, M. S., & Trumbore, S. E. (2015). Long-term controls on soil organic carbon with depth and time: A case study from the Cowlitz River chronosequence, WA USA. *Geoderma*, *247–248*, 73–87. https://doi.org/10.1016/j.geoderma.2015.02.005

Lehmann, J., Hansel, C. M., Kaiser, C., Kleber, M., Maher, K., Manzoni, S., Nunan, N., Reichstein, M., Schimel, J. P., Torn, M. S., Wieder, W. R., & Kögel-Knabner, I. (2020). Persistence of soil organic carbon caused by functional complexity. *Nature Geoscience*, *13*, 529–534. https://doi.org/10.1038/s41561-020-0612-3

Lenth, R. (2019). emmeans: Estimated marginal means, aka least-squares means. R package version 1.4.3.01 ed.

Levin, I., & Kromer, B. (1997). Twenty years of atmospheric $^{14}CO_2$ observations at Schauinsland station, Germany. *Radiocarbon*, *39*, 14.

Levin, I., Kromer, B., & Hammer, S. (2013). Atmospheric $\Delta^{14}CO_2$ trend in Western European background air from 2000 to 2012. *Tellus B: Chemical and Physical Meteorology*, *65*, 20092.

Liu, Y., He, N., Wen, X., Xu, L., Sun, X., Yu, G., Liang, L., & Schipper, L. A. (2018). The optimum temperature of soil microbial respiration: Patterns and controls. *Soil Biology and Biochemistry*, *121*, 35–42. https://doi.org/10.1016/j.soilbio.2018.02.019

Lüdecke, D. (2018). ggeffects: Tidy data frames of marginal effects from regression models. *Journal of Open Source Software*, *3*, 772. https://doi.org/10.21105/joss.00772

Luo, Z., Luo, Y., Wang, G., Xia, J., & Peng, C. (2020). Warming-induced global soil carbon loss attenuated by downward carbon movement. *Global Change Biology*, *26*, 7242–7254. https://doi.org/10.1111/gcb.15370

Malik, A. A., Chowdhury, S., Schlager, V., Oliver, A., Puissant, J., Vazquez, P. G., Jehmlich, N., von Bergen, M., Griffiths, R. I., & Gleixner, G.

(2016). Soil fungal: Bacterial ratios are linked to altered carbon cycling. *Frontiers in Microbiology*, *7*, 1247. https://doi.org/10.3389/fmicb.2016.01247

Marin-Spiotta, E., Chadwick, O. A., Kramer, M., & Carbone, M. S. (2011). Carbon delivery to deep mineral horizons in Hawaiian rain forest soils. *Journal of Geophysical Research*, *116*. https://doi.org/10.1029/2010JG001587

Marin-Spiotta, E., Silver, W. L., Swanston, C. W., & Ostertag, R. (2009). Soil organic matter dynamics during 80 years of reforestation of tropical pastures. *Global Change Biology*, *15*, 1584–1597. https://doi.org/10.1111/j.1365-2486.2008.01805.x

Marín-Spiotta, E., Swanston, C. W., Torn, M. S., Silver, W. L., & Burton, S. D. (2008). Chemical and mineral control of soil carbon turnover in abandoned tropical pastures. *Geoderma*, *143*, 49–62. https://doi.org/10.1016/j.geoderma.2007.10.001

Masiello, C. A., Chadwick, O. A., Southon, J., Torn, M. S., & Harden, J. W. (2004). Weathering controls on mechanisms of carbon storage in grassland soils. *Global Biogeochemical Cycles*, *18*. https://doi.org/10.1029/2004GB002219

Mathieu, J. A., Hatte, C., Balesdent, J., & Parent, E. (2015). Deep soil carbon dynamics are driven more by soil type than by climate: A worldwide meta-analysis of radiocarbon profiles. *Global Change Biology*, *21*, 4278–4292. https://doi.org/10.1111/gcb.13012

Megonigal, J. P., Hines, M., & Visscher, P. (2004). Anaerobic metabolism: Linkages to trace gases and aerobic processes. In W. H. Schlesinger (Ed.), *Biogeochemistry*. Elsevier-Pergamon.

Miltner, A., Bombach, P., Schmidt-Brücken, B., & Kästner, M. (2011). SOM genesis: Microbial biomass as a significant source. *Biogeochemistry*, *111*, 41–55. https://doi.org/10.1007/s10533-011-9658-z

Poeplau, C., Don, A., & Schneider, F. (2021). Roots are key to increasing the mean residence time of organic carbon entering temperate agricultural soils. *Global Change Biology*, *27*(19), 4921–4934. https://doi.org/10.1111/gcb.15787

Porras, R. C., Hicks Pries, C. E., McFarlane, K. J., Hanson, P. J., & Torn, M. S. (2017). Association with pedogenic iron and aluminum: Effects on soil organic carbon storage and stability in four temperate forest soils. *Biogeochemistry*, *133*, 333–345. https://doi.org/10.1007/s10533-017-0337-6

R Core Team. (2020). *R: A language and environment for statistical computing*. R Foundation for Statistical Computing. Retrieved from https://www.R-project.org/

Rasmussen, C., Heckman, K., Wieder, W. R., Keiluweit, M., Lawrence, C. R., Berhe, A. A., Blankinship, J. C., Crow, S. E., Druhan, J. L., Hicks Pries, C. E., Marin-Spiotta, E., Plante, A. F., Schädel, C., Schimel, J. P., Sierra, C. A., Thompson, A., & Wagai, R. (2018). Beyond clay: Towards an improved set of variables for predicting soil organic matter content. *Biogeochemistry*, *137*, 297–306. https://doi.org/10.1007/s10533-018-0424-3

Reichenbach, M., Fiener, P., Garland, G., Griepentrog, M., Six, J., & Doetterl, S. (2021). The role of geochemistry in organic carbon stabilization against microbial decomposition in tropical rainforest soils. *Soil*, *7*, 453–475. https://doi.org/10.5194/soil-7-453-2021

Reimer, P. J., Bard, E., Bayliss, A., Beck, J. W., Blackwell, P. G., Ramsey, C. B., Buck, C. E., Cheng, H., Edwards, R. L., Friedrich, M., Grootes, P. M., Guilderson, T. P., Haflidason, H., Hajdas, I., Hatté, C., Heaton, T. J., Hoffmann, D. L., Hogg, A. G., Hughen, K. A., … van der Plicht, J. (2013). IntCal13 and Marine13 radiocarbon age calibration curves 0–50,000 years cal BP. *Radiocarbon*, *55*, 1869–1887. https://doi.org/10.2458/azu_js_rc.55.16947

Rocci, K. S., Lavallee, J. M., Stewart, C. E., & Cotrufo, M. F. (2021). Soil organic carbon response to global environmental change depends on its distribution between mineral-associated and particulate organic matter: A meta-analysis. *Science of The Total Environment*, 148569. https://doi.org/10.1016/j.scitotenv.2021.148569

Sanderman, J., Hengl, T., & Fiske, G. J. (2017). Soil carbon debt of 12,000 years of human land use. *Proceedings of the National Academy of Sciences of the United States of America*, *114*, 9575–9580. https://doi.org/10.1073/pnas.1706103114

Schaetzl, R., & Anderson, S. (2005). *Soils: Genesis and geomorphology*. Cambridge University Press.

Schimel, J. (2021). The democracy of dirt: Relating micro-scale dynamics to macro-scale ecosystem function. In C. J. Hurst (Ed.), *Microbes: The foundation stone of the biosphere* (pp. 89–102). Springer.

Schlesinger, W. H. (1990). Evidence from chronosequence studies for a low carbon2storage potential of soil. *Nature*, *348*, 232–234.

Schrumpf, M., Kaiser, K., Guggenberger, G., Persson, T., Kögel-Knabner, I., & Schulze, E. D. (2013). Storage and stability of organic carbon in soils as related to depth, occlusion within aggregates, and attachment to minerals. *Biogeosciences*, *10*, 1675–1691. https://doi.org/10.5194/bg-10-1675-2013

Shi, Z., Allison, S. D., He, Y., Levine, P. A., Hoyt, A. M., Beem-Miller, J., Zhu, Q., Wieder, W. R., Trumbore, S., & Randerson, J. T. (2020). The age distribution of global soil carbon inferred from radiocarbon measurements. *Nature Geoscience*, *13*, 555–559. https://doi.org/10.1038/s41561-020-0596-z

Shi, Z., Crowell, S., Luo, Y., & Moore, B. 3rd (2018). Model structures amplify uncertainty in predicted soil carbon responses to climate change. *Nature Communications*, *9*, 2171. https://doi.org/10.1038/s41467-018-04526-9

Shukla, P., Skea, J., Calvo Buendia, E., Masson-Delmotte, V., Pörtner, H., Roberts, D., Zhai, P., Slade, R., Connors, S., & Van Diemen, R. (2019). IPCC, 2019: Climate Change and Land: An IPCC special report on climate change, desertification, land degradation, sustainable land management, food security, and greenhouse gas fluxes in terrestrial ecosystems.

Sierra, C. A., Crow, S. E., Heimann, M., Metzler, H., & Schulze, E.-D. (2021). The climate benefit of carbon sequestration. *Biogeosciences*, *18*, 1029–1048. https://doi.org/10.5194/bg-18-1029-2021

Sierra, C. A., Hoyt, A. M., He, Y., & Trumbore, S. E. (2018). Soil organic matter persistence as a stochastic process: Age and transit time distributions of carbon in soils. *Global Biogeochemical Cycles*, *32*, 1574–1588. https://doi.org/10.1029/2018GB005950

Sierra, C., Trumbore, S., Davidson, E. A., Frey, S., Savage, K., & Hopkins, F. (2012). Predicting decadal trends and transient responses of radiocarbon storage and fluxes in a temperate forest soil. *Biogeosciences*, *9*, 3013–3028. https://doi.org/10.5194/bg-9-3013-2012

Six, J., Elliott, E., Paustian, K., & Doran, J. (1998). Aggregation and soil organic matter accumulation in cultivated and native grassland soils. *Soil Science Society of America Journal*, *62*, 1367–1377. https://doi.org/10.2136/sssaj1998.03615995006200050032x

Six, J., Paustian, K., Elliott, E. T., & Combrink, C. (2000). Soil structure and organic matter I. Distribution of aggregate-size classes and aggregate-associated carbon. *Soil Science Society of America Journal*, *64*, 681–689. https://doi.org/10.2136/sssaj2000.642681x

Slessarev, E., Lin, Y., Bingham, N., Johnson, J., Dai, Y., Schimel, J., & Chadwick, O. (2016). Water balance creates a threshold in soil pH at the global scale. *Nature*, *540*, 567–569. https://doi.org/10.1038/nature20139

Sollins, P., Glassman, C., Paul, E., Swanston, C., Lajtha, K., Heil, J., & Elliot, E. (1999). Soil carbon and nitrogen. In G. P. Roberston, D. C. Coleman, C. S. Bledsoe, & P. Sollins (Eds.), *Standard soil methods for long-term ecological research* (pp. 89–105). Oxford University Press.

Soong, J. L., Castanha, C., Hicks Pries, C. E., Ofiti, N., Porras, R., Riley, W. J., Schmidt, M. W. I., & Torn, M. S. (2021). Five years of whole-soil warming led to loss of subsoil carbon stocks and increased CO_2 efflux. *Science Advances*, *7*(21), eabd1343.

Soong, J. L., & Nielsen, U. N. (2016). The role of microarthropods in emerging models of soil organic matter. *Soil Biology and Biochemistry*, *102*, 37–39. https://doi.org/10.1016/j.soilbio.2016.06.020

Soudzilovskaia, N. A., Vaessen, S., Barcelo, M., He, J., Rahimlou, S., Abarenkov, K., Brundrett, M. C., Gomes, S. I., Merckx, V., & Tedersoo, L. (2020). FungalRoot: Global online database of plant

mycorrhizal associations. *New Phytologist*, *227*, 955–966. https://doi.org/10.1111/nph.16569

Spycher, G., Sollins, P., & Rose, S. (1983). Carbon and nitrogen in the light fraction of a forest soil: Vertical distribution and seasonal patterns. *Soil Science*, *135*, 79–87. https://doi.org/10.1097/00010694-198302000-00002

Sulman, B. N., Harden, J., He, Y., Treat, C., Koven, C., Mishra, U., O'Donnell, J. A., & Nave, L. E. (2020). Land use and land cover affect the depth distribution of soil carbon: Insights from a large database of soil profiles. *Frontiers in Environmental Science*, *8*. https://doi.org/10.3389/fenvs.2020.00146

Swanston, C. W., Torn, M. S., Hanson, P. J., Southon, J. R., Garten, C. T., Hanlon, E. M., & Ganio, L. (2005). Initial characterization of processes of soil carbon stabilization using forest stand-level radiocarbon enrichment. *Geoderma*, *128*, 52–62. https://doi.org/10.1016/j.geoderma.2004.12.015

Swift, M. J., Heal, O. W., Anderson, J. M., & Anderson, J. (1979). *Decomposition in terrestrial ecosystems*. University of California Press.

Tang, J., Mo, Y., Zhang, J., & Zhang, R. (2011). Influence of biological aggregating agents associated with microbial population on soil aggregate stability. *Applied Soil Ecology*, *47*, 153–159. https://doi.org/10.1016/j.apsoil.2011.01.001

Todd-Brown, K., Zheng, B., & Crowther, T. W. (2018). Field-warmed soil carbon changes imply high 21st-century modeling uncertainty. *Biogeosciences*, *15*, 3659–3671. https://doi.org/10.5194/bg-15-3659-2018

Torn, M. S., Trumbore, S. E., Chadwick, O. A., Vitousek, P. M., & Hendricks, D. M. (1997). Mineral control of soil organic carbon storage and turnover. *Nature*, *389*, 170. https://doi.org/10.1038/38260

Trumbore, S. (2009). Radiocarbon and soil carbon dynamics. *Annual Review of Earth and Planetary Sciences*, *37*, 47–66. https://doi.org/10.1146/annurev.earth.36.031207.124300

Trumbore, S. E., & Zheng, S. (1996). Comparison of fractionation methods for soil organic matter ^{14}C analysis. *Radiocarbon*, *38*, 219–229.

van Gestel, N., Shi, Z., van Groenigen, K. J., Osenberg, C. W., Andresen, L. C., Dukes, J. S., Hovenden, M. J., Luo, Y., Michelsen, A., Pendall, E., Reich, P. B., Schuur, E. A. G., & Hungate, B. A. (2018). Predicting soil carbon loss with warming. *Nature*, *554*, E4–E5. https://doi.org/10.1038/nature25745

Villarino, S. H., Pinto, P., Jackson, R. B., & Piñeiro, G. (2021). Plant rhizodeposition: A key factor for soil organic matter formation in stable fractions. *Science Advances*, *7*, eabd3176. https://doi.org/10.1126/sciadv.abd3176

von Fromm, S. F., Hoyt, A. M., Lange, M., Acquah, G. E., Aynekulu, E., Berhe, A. A., Haefele, S. M., McGrath, S. P., Shepherd, K. D., Sila, A. M., Six, J., Towett, E. K., Trumbore, S. E., Vågen, T.-G., Weullow, E., Winowiecki, L. A., & Doetterl, S. (2021). Continental-scale controls on soil organic carbon across sub-Saharan Africa. *Soil*, *7*, 305–332. https://doi.org/10.5194/soil-7-305-2021

von Lützow, M., Kögel-Knabner, I., Ekschmitt, K., Flessa, H., Guggenberger, G., Matzner, E., & Marschner, B. (2007). SOM fractionation methods: Relevance to functional pools and to stabilization mechanisms. *Soil Biology and Biochemistry*, *39*, 2183–2207. https://doi.org/10.1016/j.soilbio.2007.03.007

Wagai, R., Kajiura, M., & Asano, M. (2020). Iron and aluminum association with microbially processed organic matter via meso-density aggregate formation across soils: Organo-metallic glue hypothesis. *Soil*, *6*, 597–627. https://doi.org/10.5194/soil-6-597-2020

Wagai, R., Mayer, L. M., & Kitayama, K. (2009). Nature of the "occluded" low-density fraction in soil organic matter studies: A critical review. *Soil Science and Plant Nutrition*, *55*, 13–25. https://doi.org/10.1111/j.1747-0765.2008.00356.x

SUPPORTING INFORMATION

Additional supporting information may be found in the online version of the article at the publisher's website.

How to cite this article: Heckman, K., Hicks Pries, C. E., Lawrence, C. R., Rasmussen, C., Crow, S. E., Hoyt, A. M., von Fromm, S. F., Shi, Z., Stoner, S., McGrath, C., Beem-Miller, J., Berhe, A. A., Blankinship, J. C., Keiluweit, M., Marín-Spiotta, E., Monroe, J. G., Plante, A. F., Schimel, J., Sierra, C. A., … Wagai, R. (2022). Beyond bulk: Density fractions explain heterogeneity in global soil carbon abundance and persistence. *Global Change Biology*, 28, 1178–1196. https://doi.org/10.1111/gcb.16023